OPTIMAL RESOURCE ALLOCATION FOR LTE UPLINK SCHEDULING IN SMART GRID COMMUNICATIONS

by

Jian Li

B.Sc., North China University of Technology, China, 2011

A thesis

presented to Ryerson University

in partial fulfillment of the

requirements for the degree of

Master of Applied Science

in the Program of

Computer Networks

Toronto, Ontario, Canada, 2013

Author's Declaration

I hereby declare that I am the sole author of this thesis.

I authorize Ryerson University to lend this thesis to other institutions or individuals for the purpose of scholarly research.

Author's Signature: _____

I further authorize Ryerson University to reproduce this thesis by photocopying or other means, in total or in part, at the request of other institutions or individuals for the purpose of scholarly research.

Author's Signature: _____

Abstract

Optimal Resource Allocation for LTE Uplink Scheduling in Smart Grid Communications

Master of Applied Science
Program of Computer Networks
Department of Electrical and Computer Engineering
Ryerson University

The success of the smart grid greatly depends on the advanced communication architectures. An advanced smart grid network should satisfy the future demands of the electric systems in terms of reliability and latency. The latest 4th-generation (4G) wireless technology, Long Term Evolution (LTE), is a promising choice for smart grid wide area networks, due to its higher data rates, lower latency and larger coverage. However, LTE is not a dedicated technology invented for smart grid, and it does not provide Quality of Service (QoS) guarantee to the smart grid applications. In this thesis, we propose an optimal LTE uplink scheduling scheme to provide scheduling time guarantee at the LTE base station for different class of traffic, with a minimal number of total resource blocks. A lightweight heuristic algorithm is proposed to obtain the optimal allocation of resource blocks for each class of traffic. The simulation results demonstrate that the proposed optimal scheduling scheme can use less resource blocks to satisfy the scheduling time requirements, compared to the two existing scheduling schemes (the Large-Metric-First scheduling scheme and the

Guaranteed Bit Rate (GBR)/Non-GBR scheduling scheme). As the multi-cell network system, the network performance of LTE may be still deteriorated by load imbalance. The unbalanced load among multiple cells leads to higher delay and higher packet drop rate in the higher-loaded cell, or an underutilization of resources in the lower-loaded cell. In order to solve this problem, a LTE load balancing algorithm is proposed aiming at finding the optimal handover operations between the overloaded cell and possible target cells. The simulation results show that the proposed load balancing algorithm can relieve network resources overload and increase the network bandwidth efficiency.

Acknowledgement

I would like to take the opportunity to express my gratitude to my supervisor, Dr. Yifeng He and Prof. Ling Guan for their tremendous guidance and kind supports throughout the duration of my graduate studies.

I would like to acknowledge the Computer Networks Department and the School of Graduate Studies at Ryerson University for their support in terms of financial aid, and work experience as a graduate assistant. Thanks to Dr. Bobby Ma for his overall guidance throughout my Master of Applied Science duration. Thanks to Mr. Arseny Taranenko to help us setup and manage the lab environment. Thanks to Dr. Xiaoli Li for her excellent assistances.

I received a lot of support during the THESL-RUCUE project. I would like to thank all members working in this group. It was an unforgettable opportunity for me to work together. I would like also thank all colleagues of Ryerson Multimedia Research Laboratory; I extend my sincere appreciation for their support and valuable suggestions on various technical aspects and sharing some lighter moments whenever required.

I would also like to thank my defense committee for taking the time and effort to review my work and provide me with their insightful comments.

I can never find the words to thank my beloved father and mother. Without them, I could never reach my current stage in life. I never felt alone with their kind support and encourages.

Contents

List of Figures

List of Tables

Chapter 1

Introduction

1.1 Smart Grid Communications

The smart grid is a modern electric system, which uses sensors, automation, computers and other application-specific devices to control and monitor the grid system. Figure 1.1 shows the conceptual diagram in smart grid communications. Currently, the constant improvements of smart grid technology have made a great progress on flexibility, security, reliability and efficiency of the electricity system. Meanwhile, the advanced systems and devices generate a large volume of traffic flows, which place a high challenge on real-time communications. Therefore, an advanced and efficient smart grid communication network is desired to satisfy demands of smart grid.

Smart grid communication architecture consists of three interconnected networks, which are Wide Area Network (WAN), Neighborhood Area Network (NAN), and Home Area Network (HAN) [1]. Each network has different operational requirements in terms of reliability and latency. As a core role in smart grid networks, the WAN is the main backbone of the network, connecting various NANs and forms a connected, integrated and robust smart grid system. The performance of WAN directly affects the system monitoring and controlling, or even the operations of the whole electric system. Therefore, the WAN layer requires a high bandwidth and a very high reliability. The WAN is often made up of fiber or

Power Line Carrier links [2]. The NAN is a high capacity, multi-purpose network, which provides connectivity to data collectors, and distribution automation equipment in smart grid network. The NAN aggregates the data from HANs, which connect in-home devices or other applications. The HAN is the internal network for different systems in the distribution system. It does not have the same capacity requirements as the NAN, but must be able to penetrate buildings to reach devices, such as Plug-in Hybrid Electric Vehicle (PHEV) and Community Energy Storage (CES) [3] [4]. HANs are typically wireless networks, and are highly optimized to utilize unlicensed radio spectrum. Descriptions of WAN, NAN, and HAN are summarized in Table 1.1.

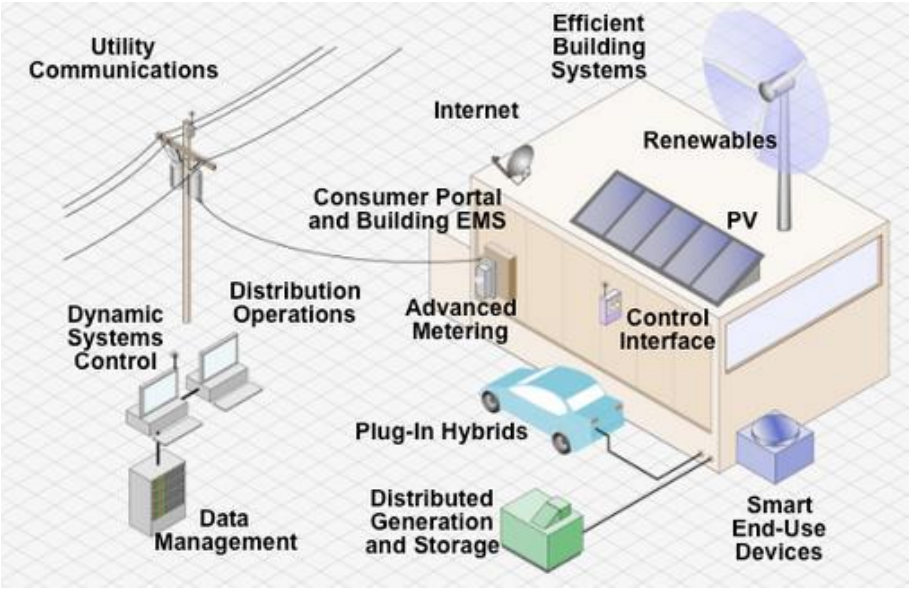

Figure 1.1 Conceptual diagram in smart grid communications

Standardized solutions, such as Long Term Evolution (LTE), Worldwide Interoperability for Microwave Access (WiMAX), Wi-Fi and ZigBee, are generally favoured in smart grid communications because they are designed for general purposes. Compared with other technologies, the latest 4th-generation (4G) wireless technology, the 3rd Generation Partnership Project (3GPP) LTE is a promising option for smart grid WAN [5]. Wi-Fi and ZigBee are standards for short-range wireless networking applications, which are widely

used in setting up indoor home/building area networks, wireless sensor networks, and smart meter networks. This thesis focuses on smart grid WAN. Therefore, we consider long-range wireless solutions. Some of sophisticated technologies such as Evolved High-Speed Packet Access (HSPA+) could be applied to WAN. However, it is expected that most utilities will be applying 4G standards in their smart grid initiatives. WiMAX and LTE are the two contenders for 4G cellular networks as well as smart grid communication networks.

Compared with WiMAX, LTE is designed for backward-compatibility with previous generations of 3GPP standards, and LTE base stations can use existing 3G towers to reduce the cost of network upgrade. Meanwhile, LTE has been truly deployed by Internet Service Provider (ISP) in Canada, United States, and other countries [6]. The Canadian government has even allocated a 30MHz frequency spectrum in 1.8GHz for smart grid application [7]. Figure 1.2 shows the role of LTE in smart grid communication networks. LTE would be a key component in the smart grid communication infrastructure for data acquisition, monitoring, control and protection.

Table 1.1 Description of smart grid network layer

Network Layer	**Description**
WAN	A WAN is the network that covers a broad area (i.e., cross metropolitan, regional, or national boundaries). The backbone of the central network for data communication is typically made of fiber.
NAN	A NAN connects various data concentrators to the local control points and/or substations. NAN can use either wired technologies, such as broadband-over-power-line or dedicated fiber, or wireless technologies, including licensed point-to-point or an unlicensed municipal Wi-Fi mesh.
HAN	HANs are the communication networks that connect each independent system component throughout the distribution system. Over the entire distribution system, there are many HANs, which are ultimately linked to the NAN and then the WAN. HANs typically use unlicensed radio spectrum for communications.

1.2 Long Term Evolution (LTE)

The term “LTE” is the abbreviation of 3GPP Long Term Evolution, which is the latest standard for the mobile communication network [8]. 3GPP is currently the dominant specification development group for mobile radio systems in the world. 3GPP technologies-Global System for Mobile Communications (GSM)/Enhanced Data rates for GSM Evolution (EDGE) and Wideband Code Division Multiple Access (WCDMA)/High Speed Packet Access (HSPA) are currently serving nearly 90% of the global mobile subscribers [9]. Figure 1.3 shows the evolution track of 3GPP development. Three multiple access technologies are evident. The ‘Second Generation’, GSM, General packet radio service (GPRS) and EDGE family were based on Time Division Multiple Access (TDMA) and Frequency Division Multiple Access (FDMA). The ‘Third Generation’, Universal Mobile Telecommunications System (UMTS) family marked the entry of Code Division Multiple Access (CDMA) into the 3GPP evolution track, known as Wideband CDMA (WCDMA). Finally LTE adopted Orthogonal Frequency Division Multiplexing (OFDM), which is the access technology dominating the latest evolutions of all mobile radio standards.

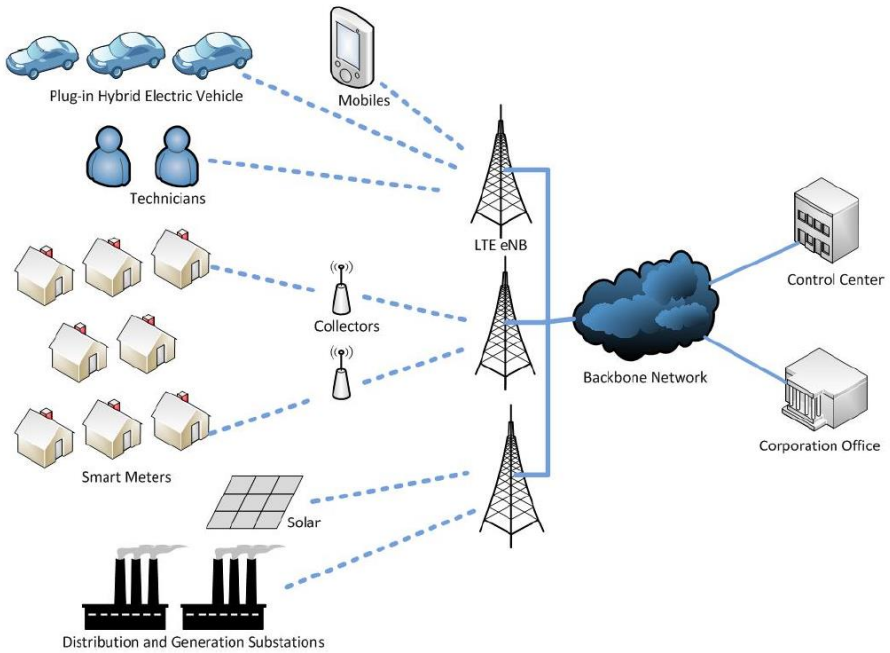

Figure 1.2 The smart grid connectivity supported by LTE

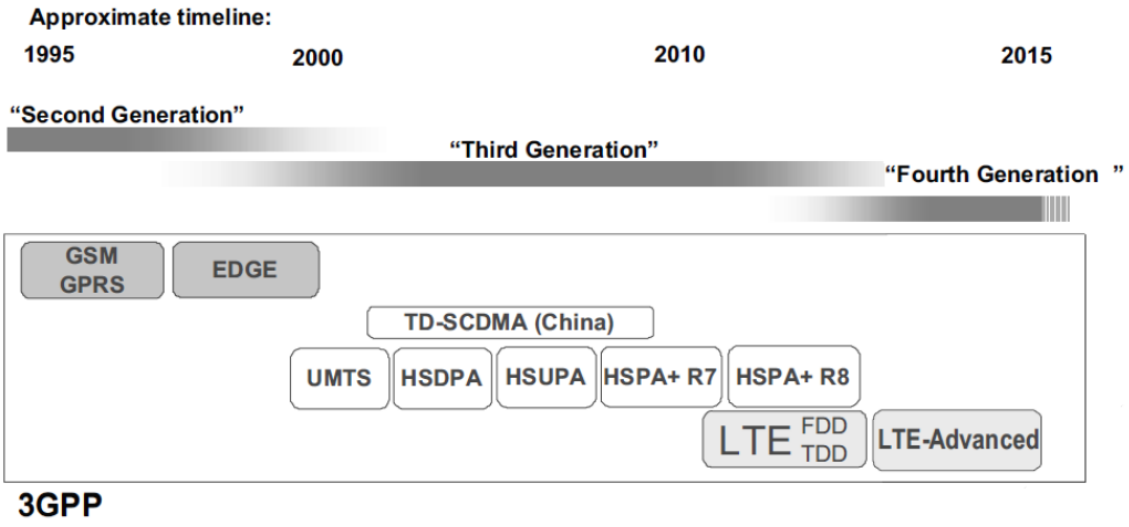

Figure 1.3 Evolutions of the mobile communications standards

The 3GPP specifications are defined in documents, which are divided into releases, where each release has a set of new features. The work on 3G LTE started with a feasibility study in December 2004, which was finalized for inclusion in 3GPP release 7. The LTE core specifications were then included in release 8. LTE is also referred to as EUTRA (Evolved UMTS Terrestrial Radio Access) or E-UTRAN (Evolved UMTS Terrestrial Radio Access Network). The thesis is carried out on the base of LTE Release 8.

Stringent requirements and targets are defined by 3GPP in the beginning of the specifications, and have been captured in 3GPP document, TR 25.913. Some key requirements and capability targets in LTE release 8 are summarized as follows:

- Data rate: Instantaneous downlink peak data rate of 100 Mb/s within a 20MHz downlink spectrum allocation, and uplink peak data rate of 50 Mb/s within a 20 MHz uplink spectrum allocation.
- Spectrum efficiency: In a loaded network, target for downlink average user throughput per MHz is 3-4 times, and for uplink is 2-3 times better than release 6.
- Latency: The one-way transmission time from the user to the server shall be less than 5 msec.

- Spectrum allocation: Operation in paired spectrum (e.g., Frequency Division Duplex (FDD) mode) and unpaired spectrum (e.g., Time Division Duplex (TDD) mode) is possible.
- Bandwidth: Saleable bandwidths of 5, 10, 15, 20 MHz shall be supported in both the uplink and downlink.
- Interworking: Interworking with existing UMTS Terrestrial Radio Access Network (UTRAN) systems and non-3GPP systems shall be ensured.
- Coverage: Throughput, spectrum efficiency and mobility targets above should met for 5km cells, and with a slight degradation for 30km cells.
- User capacity: At least 200 users per cell should be supported in an active state for spectrum allocations up to 5MHz.

The LTE, as one of the latest steps in an advancing series of mobile telecommunications systems, can be seen to provide a further evolution of functionality, increased speed and improved performance comparing to the third generation systems. The specifications of four popular technologies published by 3GPP at various times are illustrated in Table 1.2.

Table 1.2 Comparison between LTE and UMTS/3GPP 3G specifications [10]

	WCDMA	HSPA	HSPA+	LTE
Max downlink speed (bps)	384k	14M	28M	100M
Max uplink speed (bps)	128k	5.7M	11M	50M
Latency (round trip time trip time)	150ms	100ms	50ms	10ms
Mote recent 3GPP release	Rel. 99/4	Rel. 5/6	Rel. 7	Rel. 8
Date of initial roll out	2003/4	2005/6	2008/9	2009/10
Access methodology	CDMA	CDMA	CDMA	OFDMA/SC-FDMA

1.3 Challenges

Wireless communication nowadays is a fast-growing technology, and as the latest wireless communication technology, LTE becomes one promising option for smart grid communications. However, LTE is not a dedicated technology invented for smart grid. Smart

grid applications have more stringent latency requirements in WAN than other public applications such as web.

In an ideal world, it would be possible to send data over a network and gain the same performance as the data achieved by a circuit switched network [11]. However, the nature of packet data means that the same channels are used for data travelling to and from a variety of different sources and end devices. Latency is a measure of the time that it takes for data from the source to the destination of the network, and is critical for applications that use real-time communications. Latency comprises the length of time that a data package takes from the sender to the receiver. A loss or an excessive latency of the critical data, such as control messages or exceptional messages, may delay the power measurements and control, which may lead to severe economic and social consequences. Therefore, Quality of Service (QoS) mechanisms need to be deployed to guarantee the reliable and prompt delivery of critical data. In smart grid communication networks, an excessive latency of the critical data may delay the power restoration, which may lead to severe economic and social consequences. Reducing latency becomes one of significant challenge in smart grid communication networks.

LTE uplink scheduler is a key component for LTE communication. The algorithm of scheduler determines the performance of LTE processing time. Because the 3GPP LTE does not define a specific scheduling algorithm, the LTE scheduling becomes a hot topic. A large number of researchers are working on LTE scheduler, but few researchers focus on the LTE for smart grid communications. In the next generation smart grid network, LTE will be implemented into WAN and NAN. In order to achieve the high demand of smart grid applications, it is necessary to propose a proper LTE scheduling algorithm specified in smart grid network. An optimal LTE network establishes the foundation for an advanced robust smart grid system.

In the multi-cell wireless network, how to balance the load between the neighboring cells is also a critical issue for LTE. Even though LTE has a better network performance compared to other wireless technologies, a low-efficiency traffic distribution would degrade the network performance. An imbalanced multi-cell LTE network would suffer from the increased delay,

the decreased network throughput, or even the packet drops. Therefore, the LTE multi-cell load balancing problem needs to be considered.

1.4 Existing Work

For the usage of LTE in smart grid network, the researcher started to propose the next-generation smart grid framework using LTE as WAN or NAN when the LTE specification was published by 3GPP [12] [13]. Up to now, the LTE infrastructure and next-generation smart grid is becoming complete. Some countries, including Canada [7], have been planning to incorporate the LTE into the industry for several years. At the same time, some governments and corporations are investigating the feasibility of using the LTE in smart grid networks [5].

Regarding works on LTE uplink scheduler, many scheduling algorithms have been proposed. The research interests mostly concentrate on how to maximize the performance and how to keep the fairness among different users or different applications. The research methodologies are divided into three types: Best Effort Schedulers [14] [15] [16] [17], QoS-based Schedulers [18] [19] [20] and Power-optimizing Schedulers [21] [22], depending on different objectives. The details of the three categories of schedulers are described in Section 2.2. Most of the existing work aims to optimize the scheduling algorithm for normal applications, such as web, video and audio. The LTE scheduling for smart grid is less explored.

LTE load balancing among multiple cells is also important in research and standardization. The optimization goal is to find the optimal handover operations between the overloaded cell and a possible target cell. The existing methods [23] [24] [25] [26] aim to maximize user satisfaction by satisfying the hand-over trigger requirements and reducing the traffic congestion. Also, the researchers are trying to reduce the load balancing complexity and overhead of the solution to the problem.

1.5 Thesis Contributions

The contributions of this work are summarized as follows:

- We investigate the LTE uplink scheduling problem in smart grid WAN and propose a novel LTE uplink scheduling algorithm to optimize the allocation of resource blocks (RBs) in the LTE evolved NodeB (eNB or eNodeB) to provide scheduling time guarantee to different class of smart grid traffic. The simulation results demonstrate that the proposed optimal scheduling scheme can use less resource blocks to satisfy the scheduling time requirements, compared to the two existing scheduling schemes (the Large-Metric-First scheduling scheme and the Guaranteed Bit Rate (GBR)/Non-GBR scheduling scheme). This contribution will be presented in Chapter 3.
- For multi-cell LTE network, we proposed a load balancing algorithm for smart grid network. The experiment results in OPNET demonstrate that the proposed algorithm can reduce the overall delay by appropriately distributing the traffic load among multiple cells. This contribution will be presented in Chapter 4.

1.6 Organization of Thesis

This thesis consists of five chapters, which are briefly described as follows:

- In Chapter 1, we present an introduction to the smart grid communication networks, the overview of LTE, the challenge on WAN latency, the existing work to deal with the challenge, and the contributions of our work.
- In Chapter 2, we present the fundamentals of LTE, and the related work.
- In Chapter 3, we study a queuing model and an LTE uplink scheduling model. Based on the models, we analytically show the relationship between the scheduling time and the resource blocks to be allocated. Then, we present the problem formulation and propose a heuristic algorithm for the LTE uplink scheduler.
- In Chapter 4, we propose a load balancing algorithm for multi-cell LTE networks.
- In Chapter 5, we conclude our work and provide future research directions.

Chapter 2
Background

This chapter provides preliminary background information on various aspects of LTE system. The background provided below presents the LTE system architecture and the detail technologies at physical layer. This chapter then introduces the literature reviews on the smart grid WAN, the LTE QoS and LTE load balancing.

2.1 Technical Overview of LTE

2.1.1 Introduction

LTE system consists of an Evolved UMTS, E-UTRAN and an Evolved Packet Core (EPC) presented in Figure 2.1. E-UTRAN is chosen as the air interface of LTE, which is simply a network of base stations, eNB. There is no centralized intelligent controller, and the eNBs are normally inter-connected each other by the X2-interface and towards the core network by the S1-interface. In smart grid network, the end terminals, User Equipments (UEs), send the data packets to their eNBs via LTE radio signals. Such a connection is for a smart grid to upload the electricity usage status or make measurements of the data.

To achieve high radio spectral efficiency a multicarrier approach for multiple accesses was chosen by 3GPP. The LTE system defines Orthogonal Frequency Division Multiple Access

(OFDMA) as the access technique for the downlink communications and Single Carrier Frequency Division Multiple Access (SC-FDMA) for the uplink. OFDMA has advantages of robustness against multi-path fading, higher spectral efficiency and bandwidth scalability; and SC-FDMA makes UEs energy saving. The additional crucial technique applied in LTE is Multiple-Input-Multiple-Output (MIMO) that uses multiple transmitters and receivers to achieve a higher bit rate and a higher coverage.

The MAC (Media Access control) layer is responsible for scheduling, which is represented only in the UE and in the base station, leading to fast communication and decisions between the eNB and the UE. In UMTS, the scheduling is located in the controller. An additional part of MAC layer was added in the LTE eNB, which is responsible for the scheduling.

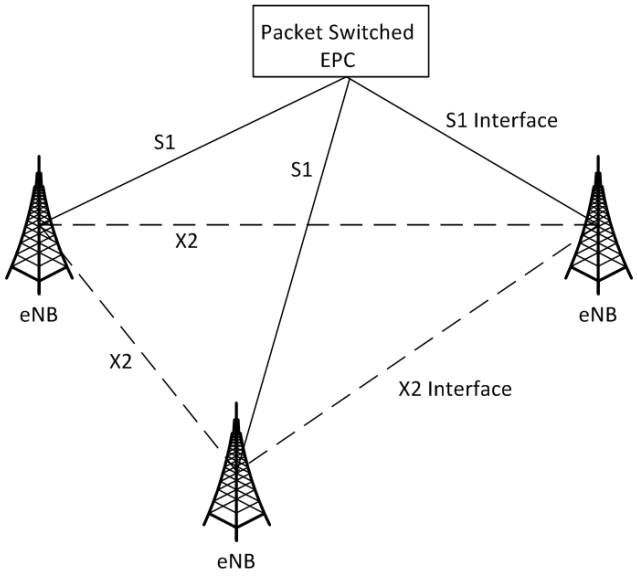

Figure 2.1 LTE architecture diagram

2.1.2 SC-FDMA and OFDMA

2.1.1.2 OFDMA

The downlink in LTE uses OFDMA for its transmission scheme. The transmitter principle in any OFDMA system is to use narrow, mutually orthogonal sub-carriers. The sub-carrier

spacing is 15 kHz regardless of the total transmission bandwidth in LTE system. Different subcarriers are grouped together to form a sub-channel that serves as the basic unit of data transmission. The main reasons why OFDMA was selected as the basic transmission scheme for LTE are its high spectral efficiency, low-complexity implementation, and the ability to easily support advanced features such as frequency selective scheduling, MIMO transmission, and interference coordination. Figure 2.2 shows the resource allocation illustration for LTE downlink.

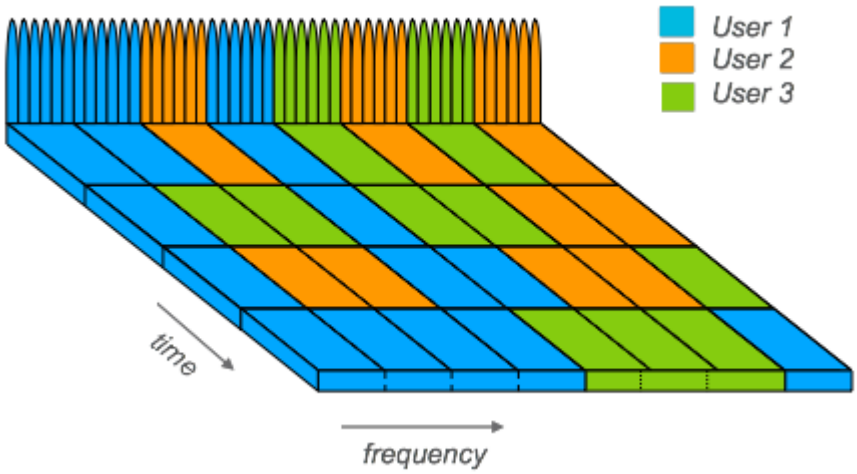

Figure 2.2 The resource allocation illustration for LTE downlink

The practical implementation of an OFDMA system is based on digital technology and more specifically on the use of Discrete Fourier Transform (DFT) and Inverse Discrete Fourier Transform (IDFT) to move between time and frequency domain representations. A basic block diagram illustrating OFDMA signal generation for one OFDM symbol is shown in Figure 2.3. Data symbols from different users are mapped to different subcarriers depending on the frequency bands assigned to those users. This is done in the frequency domain. The information is then subjected to an inverse fast Fourier transform (IFFT) to convert the frequency-domain subcarriers into time-domain signals. A cyclic prefix is then added, and the signal is ready for transmission. Note that the basic transmission unit for data is a sub-frame that spans multiple OFDM symbols. At the receiver, the reverse operation is

performed. The cyclic prefix is removed, and then the time-domain signal is subjected to a fast Fourier transform (FFT) so that the modulation symbols on each subcarrier can be extracted. Each user then extracts the frequency resource units corresponding to his assigned subcarriers. Equalization is performed and the data is passed onward for decoding.

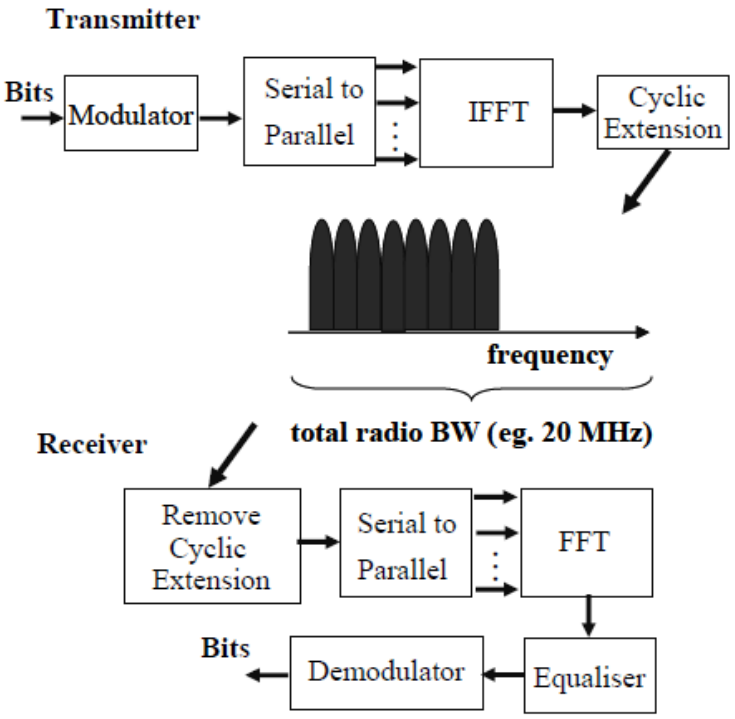

Figure 2.3 Block diagram for OFDMA

2.1.1.1 SC-FDMA

In the uplink, SC-FDMA is selected due to its ability to provide similar advantages to OFDM, such as orthogonality among users, frequency domain equalization, and robustness with respect to multipath operation. However, SC-FDMA with a lower peak-to-average power ratio (PAPR) greatly benefits the mobile terminals or users in terms of transmit power efficiency and reduced cost of the power amplifier. As a result, the average transmission power is much higher with SC-FDMA than with OFDMA. This increases coverage in the uplink and provides higher uplink data rates to users at the cell edge.

Figure 2.4 shows the resource allocation for LTE uplink. The SC-FDMA resource block for frequency domain signal generation is defined using the same values used in the OFDMA downlink, based on the 15 kHz sub-carrier spacing. Thus even if the actual transmission by name is a single carrier, the signal generation phase uses a subcarrier term. In the simplest form the minimum resource allocated uses 12 sub-carriers, and is thus equal to 180 kHz. It is obvious from the Figure 2.2 and Figure 2.4 that the two techniques transmit the same amount of data in the same time period and using the same bandwidth. However in SC-FDMA the UE needs to transmit only one wide carrier at a time containing the information of one data symbol, while in OFDMA a number of narrow sub-carriers need to be transmitted at each time period. Thus the SC-FDMA technique is more power efficient.

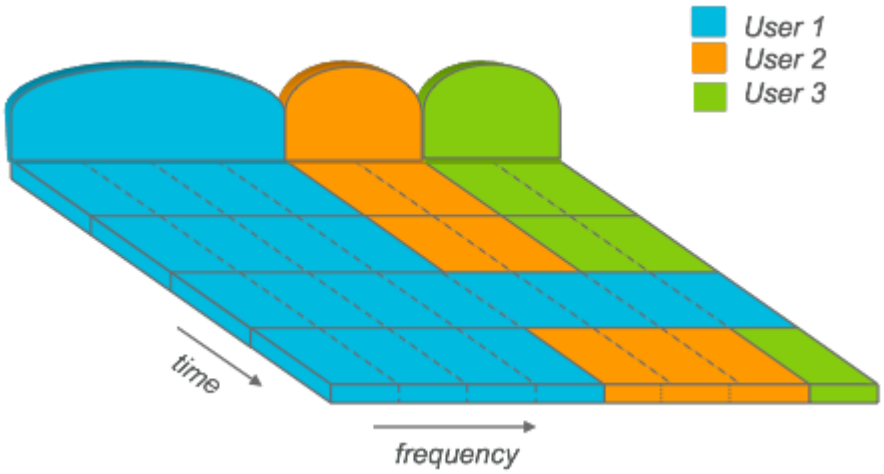

Figure 2.4 Illustration of resource allocation for LTE uplink

Frequency domain generation of the signal is shown in Figure 2.5. The frequency domain generation of the signal adds the OFDMA property of good spectral waveform in contrast to time domain signal generation with a regular Quadrature Amplitude Modulation (QAM) modulator. Thus the need for guard bands between different users can be avoided, similar to the downlink OFDMA principle. As in an OFDMA system, a cyclic prefix is also added periodically, but not after each symbol as the symbol rate is faster in the time domain than in OFDMA to the transmission to prevent inter-symbol interference and to simplify the

receiver design. The receiver still needs to deal with inter-symbol interference as the cyclic prefix now prevents inter-symbol interference between a block of symbols, and thus there will still be inter-symbol interference between the cyclic prefixes. The receiver will thus run the equalizer for a block of symbols until reaching the cyclic prefix that prevents further propagation of the inter-symbol interference.

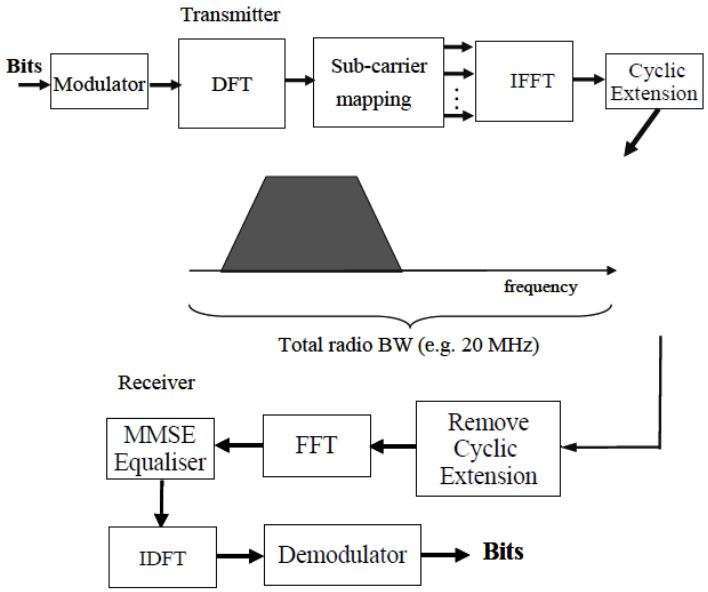

Figure 2.5 Block diagram for SC-FDMA

2.1.1.3MIMO

MIMO is used in LTE to improve the performance of the system. This technology provides LTE with the ability to further improve its data throughput and spectral efficiency above that obtained by the use of OFDM.

For the uplink from the mobile terminal to the base station, a scheme called Multi-User MIMO is employed. In Multi-user MIMO, the base station requires multiple antennas, while the mobiles terminal only needs one transmit antenna, thus considerably reducing the cost. In operation, multiple mobile terminals may transmit simultaneously on the same channel or channels, but they do not cause interference to each other because mutually orthogonal

pilot patterns are used. This technique is also referred to as Spatial Domain Multiple Access (SDMA).

For the downlink, a configuration of two transmit antennas at the base station and two receive antennas on the mobile terminal is used as baseline, although configurations with four antennas are also being considered.

2.1.3 Control signaling for uplink scheduling

Channel State Information (CSI) refers to the SINR measurement of the channel properties on the uplink direction between the UE and eNodeB. This information describes how a signal propagates from the transmitter to the receiver and represents the combined effect of, for example, scattering, fading, and power decay with distance. The CSI makes it possible to adapt transmissions to current channel conditions, which is crucial for achieving reliable communication with high data rates in multi-antenna systems.

Buffer Status Reporting (BSR) refers to the 3GPP standardized reporting mechanism that a UE uses to send its buffer information to the eNodeB [27]. BSR mechanism plays an important role in QoS provisioning. The scheduler can get a status report on how much data awaiting transmission at the UE's uplink buffer.

2.2 Literature Review

2.2.1 Related work on smart grid WAN

Traditionally, the communication infrastructure of a power system consists of supervisory control and data acquisition (SCADA) systems with dedicated communication channels between the control center and a WAN [28]. The SCADA systems connect all the major power system operational facilities, including the central generating stations, the transmission grid substations and the primary distribution substations to the System Control

Centre. The WAN is used for corporate business and market operations. These form the core communication networks of the traditional power systems. However, in the Smart Grid, it is expected that these two elements of communication infrastructure will merge into a Utility WAN.

Many investigations have been conducted in the area of smart grid WAN communications. In [12] [13], the authors presented the background and motivation of communication infrastructure in smart grid systems, and summarized the major requirements that smart grid communications must meet. The communication is characterized by the fact that most of the interactions must take place in real time, with a hard time bound, since a smart grid system might have over millions of consumers and devices. For real-time sensing/metering purposes, reading messages need to be transmitted within a very short time frame. For instance, the maximum allowed time is in the range of 12-20 milliseconds (ms), depending on the type of protection scheme which requires that the disconnection of fault current should be within approximately 100ms. Power System Control signals mainly include supervisory control of the power process on the secondary or higher levels. Measured values of these systems must not be older than 15 seconds, when arriving at the control center. Breaking information shall arrive no later than 2 seconds after the emergency event has occurred [29].

The authors in [30] addressed critical issues on smart grid technologies primarily in terms of information and communication technology issues and opportunities. Different communications technologies supported by two main communications media, i.e., wired and wireless, can be used for data transmission between smart meters and electric utilities. Wireless communications have some advantages over wired technologies in certain instances, such as low-cost infrastructure and ease of connection to difficult or unreachable areas. But the technological choice that fits one environment may not be suitable for the other. Therefore, the authors briefly explained several popular wireless technologies, such as ZigBee, GPRS, HSPA+, WiMAX, etc. in terms of their advantages and disadvantages.

The feasibility of applying LTE to smart grid communication networks was studied in [5]. The document released by the National Institute of Standard and Technologies (NIST) [31], analyzed the traffic distributions of Distribution Automation (DA) networks and concluded that the major technique challenge for the LTE DA network is the tightly coupled Radio Access Network (RAN) latency constraint of 100ms and reliability requirement of 10^{-3}. For the latency requirement, the bandwidth is reserved only for the low-duty-cycle field devices to mitigate queuing delays and decrease scheduling delay by maintaining all field devices in a Radio Resource Control-CONNECTED state. For the reliability, the simulation results show that the reliability requirement can be satisfied with 4×2 closed-loop Single User-MIMO (SU-MIMO) system in downlink, and with 1×4 system in uplink, respectively.

In [32], the authors designed communication network architecture for smart grid based on broadband wireless communication technology, such as 3G, LTE and LTE-Advanced. As the emergency communication has a critical requirement of wireless communication technology in the smart grid, a solution for emergency communications is designed based on LTE technology. In the solution, the Time-division duplex mode is used, and SC-FDMA uplink is configured with more time slot resources than OFDMA downlink.

2.2.2 Related work on LTE QoS

This section provides a survey on the existing work on LTE schedulers in the literature. Based on the schedulers' objective, the schedulers can be categorized in to three classes:

1. Best Effort Schedulers
2. QoS-Based Schedulers
3. Power-Optimized Schedulers

Best Effort Schedulers

Most of the existing work for UE uplink scheduling focused on maximizing performance metrics such as data throughput and fairness. Best-effort schedulers were designed to maximize the utilization of the radio resources and/or fairness of resource sharing among UEs.

The work in [14] proposed two new scheduling algorithms considering both the channel contiguity constraint and the latency constraint. The first greedy algorithm called a Low Cost-delay (LC-delay) algorithm, schedules each resource block to a user in a way that minimizes allowed delay and guarantees a maximum throughput for each user. It goes through each block, one after the other, and assigns it to a user, taking into account the adjacency resource block constraints, if the minimum delay and maximum throughput requirements are satisfied for all users. Otherwise, it first assigns the users with critical delay or throughput constraints, as long as resource blocks are available and adjacent resource block constraints are satisfied. Mathematically, the LC-delay algorithm is formulated as follow:

$$delay_k \leq delay_{max}, \quad k \in K \tag{2.1a}$$

$$R_k \geq R_{min} \qquad k \in K\ K \tag{2.1b}$$

where each resource block RB to a user k maximizes the marginal utility, satisfies the maximum allowed delay $delay_{max}$, and guarantees a minimum throughput R_{min} for each user. The second proposed algorithm allocates the resource block to maximize the metric value λ.

$$\lambda = \frac{delay_k}{R_k} \tag{2.2}$$

In such a way users will never experience a delay greater than the delay requirement. Proportional Fairness delay (PF-Delay) algorithm differs from the LC-Delay algorithm in the use of a different metric in assigning channels. Instead of using the marginal utility in LC-Delay algorithm, PF-Delay algorithm uses the proportion between the current throughputs to the total throughput as the metric. In addition, the resource blocks are not assigned in

order, but with respect to the user with the most critical delay requirement, under the condition that the user has a reasonable utility value.

The authors in [15] investigated the performance of frequency and time domain scheduling in LTE uplink, particularly the performance impact of various scheduling metrics aiming to achieve proportional fairness in throughput or resource allocation. Three different metrics were presented in this paper, which is shown in Table 2.1. In the table, $\hat{T}(i,n,k)$ is the estimated achievable throughput for UE *i* at scheduling interval *n* on PRB *k*; $\bar{T}(i,n)$ is the past averaged acknowledged throughput for UE *i*, at scheduling interval *n*. For PF-SINR definition, $SINR_{CSI}(i,n,k)$ represents CSI SINR measured at the BS for UE *i*, at scheduling interval *n*, on PRB *k*; $SINR_{CSI,w}(i,n)$ representes wideband CSI SINR measured at the BS for UE t at scheduling interval *n.* $\bar{T}_w(i,n)$ in PF-TTW is the estimated wideband achievable throughput for UE *i*, at scheduling interval *n*. Based on the properties exhibited by the metrics, a throughput-based Proportional Fairness (PF) metric in time domain combined with an SINR-based PF metric in frequency domain is shown to be particularly effective. Results show that such combination is able to achieve a gain of approximately 21% in average cell throughput and 37.5% in outage user throughput compared to the combination of PF both in the time domain and in the frequency domain.

The authors in [16] investigated the latency caused by LTE communication networks, and established an empirical mathematical model for the distribution of the latency. The limitations of the current LTE were discussed, and a new scheduler with a new utility function was designed, which is shown below

$$\lambda = W_p + P_{pf} \tag{2.3}$$

where W_p is the weight for the UE in the smart grid, which is obtain as

$$W_p = \alpha_1 r + \alpha_2 l + \alpha_3 q \tag{2.4}$$

with $\alpha_1 + \alpha_2 + \alpha_3 = 1$. r representing constant data updating rates; l representing equivalent data packets lengths; and q representing approximately invariant channel qualities. P_{pf} is given by the traditional LTE scheduling algorithm:

$$P_{pf} = \left(\frac{C}{I}\right)[R(t)]^{-1} \tag{2.5}$$

Here, C/I represents channel condition and $R(t)$ is the throughput within the time interval.

Table 2.1 Metric definitions

Metric name	**Definition**
PF	$\frac{\hat{T}(i,n,k)}{\bar{T}(i,n)}$
PF-SINR	$\frac{SINR_{CSI}(i,n,k)}{SINR_{CSI,w}(i,n)}$
PF-TTW	$\frac{\hat{T}(i,n,k)}{\bar{T}_w(i,n)}$

In [17], a game theoretical formulation is derived where the scheduling problem is represented as a Nash bargaining game. It was shown in the simulations that the maximization of the sum throughput leads to a higher cell throughput, while considering the logarithm of throughput as a utility function ensures proportional fairness, and thus constitutes a trade-off between throughput and fairness.

QoS-Based Schedulers

Bandwidth and QoS Aware (BQA) scheduler was proposed in [18], in which QoS provision is guaranteed to the UEs. It maximizes the cell throughput by giving priority to UEs with better channel conditions. Multi-bearer UEs are supported by the scheduler. The scheduler is time and frequency domain decoupled. Resource allocation is performed with bandwidth flexibility, contiguity constraint of subcarriers and UE buffer size consideration.

QoS-based scheduler was proposed in [19], where the authors proposed Guaranteed Bit Rate/Proportional Fairness (GBR/PF) LTE uplink scheduler accompanied by a proposal for QoS-aware algorithm. The proposed packet scheduling algorithm explicitly decouples the scheduling process into time domain and frequency domain scheduling. QoS provisioning is achieved by introducing a term that is a function of the UE's average throughput normalized by its GBR. The introduced GBR-based term is used in time domain to prioritize UEs, and is also used as part of the frequency domain metric. The study showed that the proposed scheduler can provide better support for QoS traffic streams, especially the ones with the low GBR rate, such as Voice over IP (VoIP) services.

A new uplink scheduling algorithm with a new utility function were used in [20]. The proposed uplink scheduling algorithm can distinguish between inter-class and intra-class prioritization of the multiplexed traffic for the LTE network. The results obtained by the new algorithm showed the effectiveness and strength of handling traffic priority and fairness. Moreover the interesting opportunity cost function has been used to adjust the network operator’s revenue loss. By adjusting different parameters, the scheduler can achieve its desired level of inter-class and intra-class prioritization with fairness.

Power-Optimized Schedulers

The goal of Power-optimized schedulers aims to reduce power consumption of mobile UEs on wireless transmissions. A scheduler in this category first acquires some QoS aspects of the traffic flows transmitted on the LTE uplink, such as packet delay budget or GBR requirements. The schedulers then perform some algorithmic decisions to reduce the transmission power of the UE under the constraints of QoS requirements.

Power-optimized schedulers for LTE were not investigated thoroughly in the literature. Two scheduling algorithms can be categorized into this class. The first algorithm was presented in [21], where the authors introduced power minimized schedulers based on queuing delay constraints. The idea is to make significant savings in the UE’s transmission power under satisfying the UE’s GBR requirements premise.

Another algorithm for power-based LTE uplink scheduling was proposed in [22]. The scheduler first creates a matrix to represents all the possible allocation patterns possible of uplink resource blocks under the contiguity constraint. The scheduler then calculates the power needed for each possible allocation pattern for each UE. Finally, the scheduler performs a greedy-based search algorithm to find the UE-PRB allocation pattern that minimizes the power consumption on each UE under the GBR requirements.

2.2.3 Related work on LTE load balancing

The load balancing algorithm in the wireless cellular networks aims at finding the optimum handover operations between the overloaded cell and a possible target cell. This objective assures that the users that are handed over to the target cell will improve the network improvement in terms of the latency, and make the whole network more efficient.

Many researchers are working on LTE load balancing. An early paper, [23], presented a mathematical framework for quantitative investigations of self-optimizing wireless networks for LTE system. The SINR ratio distribution, the number of satisfied users and energy efficiency were considered in presented models. A simple self-optimizing network algorithm was described in this paper, which adjusts the cell-specific handover thresholds for the sake of load balancing. This algorithm has been applied to a simple scenario where the users are concentrated in particular areas in the network. The number of unsatisfied users was significantly reduced compared with the homogenous solution.

In [24], the authors proposed a handover offset based load balancing algorithm using the parameter “cell specific offset” to force users to handover from the overload eNB to the target eNB, which improved the earlier proposed LTE load balancing algorithm in [23]. The main goal of the proposed algorithm is to find the optimum handover offset that allows the maximum number of users to change cell without any rejections by admission control mechanism at target eNB side.

In [25], a directional cell breathing based-reactive congestion control heuristic algorithm was proposed, where the coverage area of a cell sector can dynamically be extended towards a nearby loaded sector or shrunk towards cell center for a loaded sector.

In order to diminish the negative effects on handover failure, [26] proposed an algorithm which picks the best hysteresis and time-to-trigger combination for the current network status. This paper involves a handover failure ratio:

$$HPI_{HOF} = \frac{N_{HOfail}}{(N_{HOfail} + N_{HOsucc})}$$

where the handover failure ratio (HPI_{HOF}) is the ratio of the number of failed handovers (N_{HOfail}) to the number of handover attempts. The number of handover attempts is the sum of the number of successful (N_{HOsucc}).

2.3 Chapter Summary

In this chapter, section 2.1 introduces the technical overview of LTE, which is related to the LTE physical layer frame structure and control signaling. Section 2.2 presents the literature reviews of the smart grid WAN, the LTE QoS and the LTE load balancing.

Chapter 3
LTE Uplink Scheduling Algorithm for Smart Grid

This chapter presents a new LTE uplink scheduling algorithm for Smart Grid communications. First, a queuing model and an LTE uplink scheduling model are presented. Next, a lightweight heuristic algorithm is proposed to obtain the optimal allocation of resource blocks for each class of smart grid traffic. Finally, the simulation results are presented to evaluate the performance of the proposed algorithm.

3.1 Introduction

In many countries, data fiber network, synchronous optical network (SONET), SCADA network, etc., are being deployed in the current smart grid WAN. However, the smart grid WAN is still dissatisfactory in some aspects, such as lack of common backhaul medium for data communication. Furthermore, future demands including PHEV and CES require reliable two-way communications and interactivities that traditional network systems cannot provide. Therefore, the traditional communication architecture needs to be upgraded urgently, or even replaced by a more advanced communication technology.

Currently, the latest 4G wireless technology, the 3GPP LTE, is the promising option for smart grid WANs. There are several kinds of technologies available for smart grid WAN, such as LTE, WiMAX, etc. Compared with other technologies, LTE provides excellent performance in terms of higher data rates, lower latency and larger coverage. Moreover, as a wireless communication technology, LTE supplies extra flexibility than the wired communications. However, LTE is not a technology invented for smart grid. Smart grid applications have special QoS requirements such as more stringent latency requirements in WAN than other public applications such as web. An excessive delay of the critical data may delay the power restoration, which may lead to severe economic and social consequences. Reducing latency or end-to-end delay becomes one major challenge in smart grid communication networks.

In this chapter, we study the LTE uplink scheduling problem in smart grid WAN. Particularly, we optimize the allocation of RBs in the LTE eNB in LTE, to provide scheduling time guarantee to different class of smart grid traffic.

3.2 System Models

3.2.1 Queuing Model

According to the requirements, the data in the smart grid can be categorized into different classes. For example, data on remote workforce is classified into low-priority class, while the control data from the control center and exception messages such as the outage notifications are classified into the critical class. The queuing model is used to study the scheduling time of each class and the total scheduling time for the LTE scheduler. The queuing model consisting of several queues and one scheduler is involved in our study. The queuing model in LTE scheduler is shown in Figure 3.1. Assume that the scheduler provides C classes of traffic with different priorities with smaller class number corresponding to a higher priority. The traffic of class-c ($\forall c = 1,2, \dots, C$) is characterized by four parameters: 1) the arrivals of the class-c requests modeled as a Poisson Process with average arrival rate λ_c requests/second; 2) the average request size F_c Kbytes/request specified by the size of every

request; 3) the upper bound of scheduling time τ_c in seconds; and 4) the possibility ρ_c that an arriving request belongs to class-c.

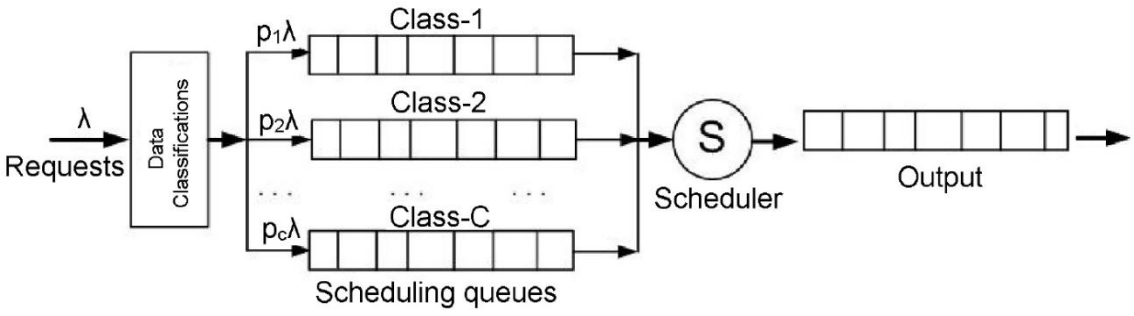

Figure 3.1 Queuing model

In order to simplify the queuing model, we assume that the model consists of C queues connecting to a scheduler, and each queue is used to hold the traffic of the corresponding class. Requests can be served immediately at the scheduling rate S_{total} by the scheduler. In this paper, we employ the preemptive priority service scheme.

In the queuing model, the scheduling rate for class-c is denoted as $S_{sch}^{(c)}$. We have $S_{total} = \sum_{c=1}^{C} S_{sch}^{(c)}$. The average size of requests of class-c is F_c. Thus, the scheduling time for class-c traffic flows is assumed to follow a Poisson distribution with mean time of $F_c/S_{sch}^{(c)}$. In accordance with the composition property of Poisson Process, the arrivals of task requests in class-c follow a Poisson Process with arrival rate $\lambda_c = \rho_c\lambda$ and the total arrivals of all requests follow a Poisson Process with average arrival rate $\lambda = \sum_{c=1}^{C} \lambda_c$. In a preemptive priority M/M/1 queuing system, the mean scheduling time for class-c data flow is given by [33]:

$$T_{sch}^{(c)} = \frac{F_c/S_{sch}^{(c)}}{1-\beta_{sch}^{(c-1)}} + \frac{\sum_{j=1}^{c}(\rho_c\lambda F_j^2/{S_{sch}^{(j)}}^2)}{(1-\beta_{sch}^{(c-1)})(1-\beta_{sch}^{(c)})} \tag{3.1}$$

where $\beta_{sch}^{(c)} = \sum_{j=1}^{c} \frac{\rho_j\lambda F_j}{S_{sch}^{(c-1)}}$. To ensure the schedule queue stable, $\beta_{sch}^{(c)} = \sum_{j=1}^{c} \frac{\rho_j\lambda F_j}{S_{sch}^{(c-1)}} < 1$ should be satisfied.

3.2.2 LTE Uplink Scheduling Model

The LTE uplink scheduler is located at the base station in LTE. The minimum transmission unit of LTE scheduler is known as a resource block. The radio resource that is available in the uplink LTE system is defined in both frequency and time domains. In the frequency domain, each RB consists of 12 consecutive subcarriers and in the time domain it is made up of one time slot of 0.5ms duration. Each 1ms Transmission Time Interval (TTI) consists of 2 slots, and a subframe is defined as 10 TTIs. At each TTI, multiple RBs can be assigned to a number of users with different classes; each resource block however can be assigned to at most one user. The LTE scheduler has B MHz bandwidth, divided into N RBs. Table 3.1 shows the channel bandwidth for a given quantity of resource blocks. We assume that the scheduler is capable of assigning RBs arbitrarily to all users and each RB n has a bandwidth of B/N. Let $n = \{1,2, \dots, N\}$ denotes the RB index set. For simplicity, we suppose that uniform power allocation across all subcarrier.

Table 3.1 Number of resource blocks for different LTE bandwidths

Channel bandwidth [MHz]	1.4	3	5	10	15	20
Number of resource blocks	6	15	25	50	75	100

We define a variable x_c to indicate the number of resource blocks assigned to class-c traffic flows. According to Shannon-Hartley theory, for uplink direction, the maximum uplink channel throughput of class-c in the SC-FDMA multiplex can be expressed as [34] [35]:

$$S_{sch}^{(c)} = x_c \frac{B}{N} \log_2(1 + SINR_n^{(c)}) \tag{3.2}$$

where $SINR_n^{(c)}$ is the average Signal to Interference and Noise Ratio (SINR) for the RB n at the transmitter. The LTE standard provides reporting mechanisms (CSI) to provide the packet

scheduler with valuable information about the cellular environment that can assist in increasing the scheduling operation in the uplink [36].

In the situation, we can define $SINR_n^{(c)}$ and evaluate for every class in each time duration, presented in [37]

$$SINR_n^{(c)} = \frac{\psi_k / L_{x(u)}(\vec{p}_u)}{\sum_{k \neq x(u)} \psi_k \cdot \rho_k / L_k(\vec{p}_u) + N} \tag{3.3}$$

where ψ_k represents the transmit power of the sender for cell *k* at time t. A user u is located at position $\vec{p}_u$. A function $x(u)$ means that user u is served by the cell $k = x(u)$.

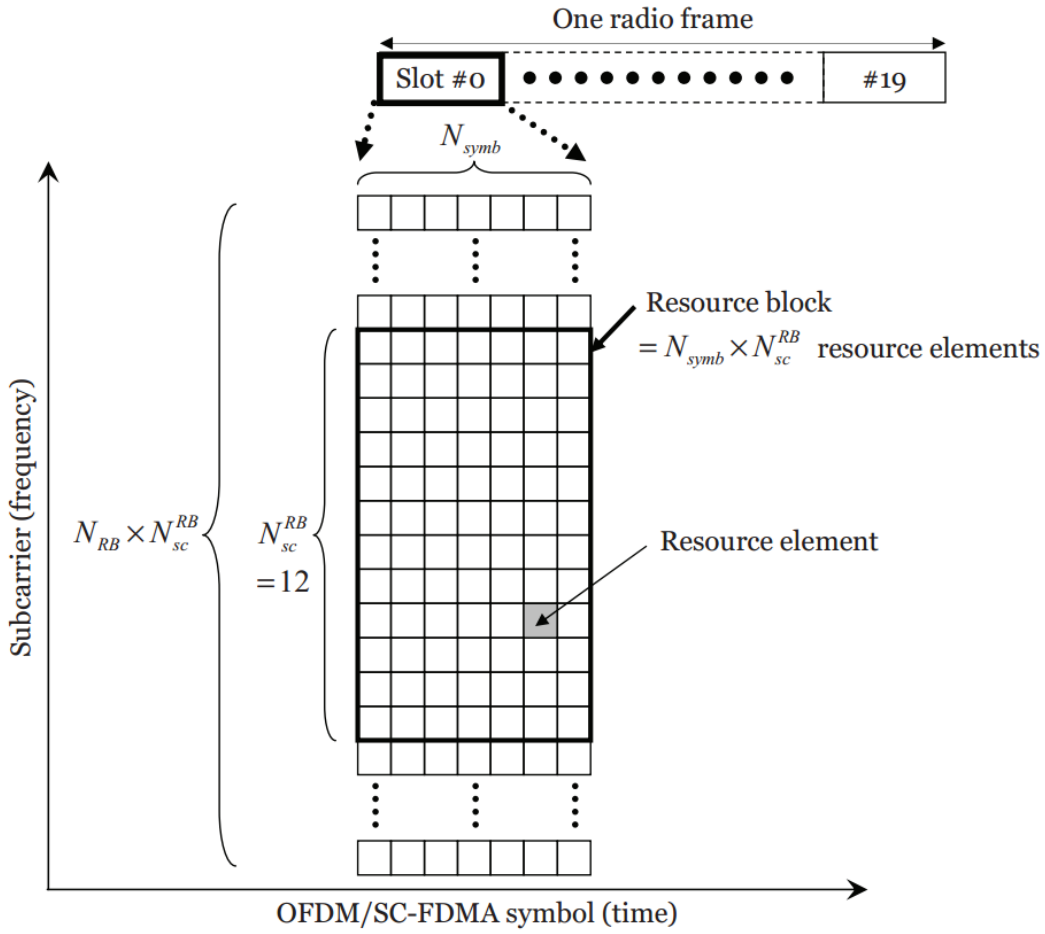

Figure 3.2 3GPP LTE radio frame structure

Each user is connected exactly to a single cell. $L_{x(u)}(\vec{p}_u)$ and $L_k(\vec{p}_u)$ donate the path loss defined by the positions of user u (taking into account the distance between them) to the currently serving cell and other interference cell, respectively.

Therefore, the total scheduling rate for the LTE uplink scheduling is given by:

$$S_{total} = \sum_{c=1}^{C} x_c \frac{B}{N} \log_2(1 + SNR_n^{(c)}) \tag{3.6}$$

Based on the above analysis, we can formulate the mean scheduling time for processing class-c traffic as follows:

$$T_{sch}^{(c)} = \frac{F_c/(x_c \frac{B}{N} \log_2\left(1 + SNR_n^{(c)}\right))}{1 - \sum_{j=1}^{c-1} \frac{\lambda_j F_j}{x_j \frac{B}{N} \log_2\left(1+SNR_n^{(j)}\right)}} +$$

$$\frac{\sum_{j=1}^{c} (\lambda_j F_j^2/(x_j \frac{B}{N} \log_2(1+SNR_n^{(c)}))^2)}{(1-\sum_{j=1}^{c-1} \frac{\lambda_j F_j}{x_j \frac{B}{N} \log_2\left(1+SNR_n^{(j)}\right)})(1-\sum_{j=1}^{c} \frac{\lambda_j F_j}{x_j \frac{B}{N} \log_2\left(1+SNR_n^{(j)}\right)})} \tag{3.7}$$

$$\forall c = 1, 2, \dots, C,$$

Therefore, the total scheduling time for processing all requests is formulated as:

$$T_{total} = \sum_{c=1}^{C} \frac{\lambda_c}{\lambda} T_{sch}^{(c)} \tag{3.8}$$

3.3 Problem Formulation

We formulate the allocated resource blocks minimization problem based on the queuing model and the LTE uplink scheduling model, aiming to minimize the total number of the allocated resource blocks while satisfying the scheduling time constrain for each class of traffic. The problem of resource block minimization can be written as:

$$\text{Minimize}_{\{x_c\}}\, x_c \tag{3.9a}$$

Subject to

$$x_c \leq N, \qquad \forall c = 1, 2, \ldots, C, \tag{3.9b}$$

$$\sum_{c=1}^{C} x_c \leq N, \tag{3.9c}$$

$$\sum_{j=1}^{c} \frac{\rho_j \lambda F_j}{S_{sch}^{(c-1)}} < 1, \tag{3.9d}$$

$$\lambda_c F_c < S_{sch}^{(c)}, \qquad \forall c = 1, 2, \ldots, C, \tag{3.9e}$$

$$T_{sch}^{(c)} < \tau_{c,} \qquad \forall c = 1, 2, \ldots, C, \tag{3.9f}$$

where Eq.(3.9b) indicates that the resource blocks assigned to class-c must be less than or equal to the total number of resource blocks, Eq. (3.9c) declares that the number of allocated resource blocks is less than the total number of resource blocks, Eq. (3.9d) presents the inequality to ensure the queuing model stability, Eq. (3.9e) shows the relationship between the arrival rate and the scheduling rate for class-c, and τ_c in Eq. (3.9f) is the upper bound of the scheduling time for class-c service which is pre-defined according to the QoS requirements for different classes.

3.4 The proposed LTE Uplink Scheduling Algorithm

Although global searching to find the solution of the minimum resource blocks could be feasible, such method is inefficient. Therefore, we propose a heuristic scheme to obtain a sub-optimal solution. The proposed heuristic scheme dynamically decides the number of resource blocks allocated to each class in each TTI. Algorithm 1 describes the proposed heuristic scheme in details. In each TTI, the eNB scheduler captures the Buffer Status Report and Channel State Information from the UEs, and calculates SINR values. The principle of the allocation is to assign RBs in sequential order from the higher-priority classes to lower-priority classes. The initial number of resource blocks to be allocated for class-c, x, is set to 1.

Next, the scheduler calculates the scheduling time $T_{sch}^{(c)}$ using Eq. (3.7) and compares it with the scheduling time requirement $\tau_{c,}$. If the value of calculation is larger than the requirement, the value x is increased by 1. The scheduler keeps increasing the resource blocks, until the scheduling time $T_{sch}^{(c)}$ meets the requirement. When the calculated value becomes smaller than τ_c, x_c is determined and the scheduler allocates x_c resource blocks to the class-c traffic flows. Then the scheduler begins to process the next class traffic flows. Once the allocation is complete, the system updates all the relevant parameters.

Note that the system adjusts itself in order to match the QoS target. The proposed allocation scheme aims to allocate minimum RBs. Our proposed heuristic can guarantee each class of traffic is allocated the minimum RBs. If any of the class obtains one less resource block, this class of traffic cannot satisfy the scheduling time requirements.

3.5 Simulations

3.5.1 Simulation Setting

In this section, we perform LTE uplink simulations to evaluate the performance of the propose scheduling scheme.

Table 3.2 summarizes the parameter settings of smart grid traffic. All traffic is divided into three classes. Class-1 traffic has the highest priority, including the exception messages and alarms. Class-2 contains the control messages which are not as critical as those in class-1. The normal operation traffic is classified into class-3. The total arrival rate of the incoming traffic is set in the range of 100-300 requests/second. The other simulation configurations can be seen in Table 3.3. We evaluate the number of RBs allocated for different classes in different scheduling algorithms as well as the performance of the algorithms in terms of scheduling time.

We compare the performances among three scheduling schemes: 1) our proposed scheduling, 2) a Large-Metric-First scheduling scheme [16], and 3) the Guaranteed Bit Rate

(GBR)/Non-GBR scheduling scheme [38]. The Large-Metric-First scheduling scheme is determined by a utility function for UEs, which is given by $\lambda = W_P + P_{PF}$, where W_P is the weight for UEs in the smart grid communication network and P_{PF} is given by traditional LTE scheduling proportional fair (PF) algorithm. The GBR/Non-GBR scheduling represents a guaranteed minimum bit rate requested by an application. In LTE, the GBR bearers and non-GBR bearers can be provided. Of these, the GBR bearers are typically used for applications such as exception messages and control messages, with an associated GBR value; higher bit rates can be allowed if resources are available. Non-GBR bearers do not guarantee any particular bit rate, which usually are used for the normal operation applications. All simulations have been conducted with the parameters described in Section 3.5.2.

Algorithm 1 Proposed LTE uplink scheduling algorithm

Let N be the set of resource blocks.
Let n be the index of resource blocks.
for $n = 1$ to N **do**
    Calculate SINR value of each resource block
end for
$n = 0$
for $c = 1$ to C **do**
    $x \leftarrow 1$
    while $n < N$ **do**
        Calculate $T_x^{(c)}$
        if $T_x^{(c)} < \tau_c$ and $\sum_{j=1}^{c} \frac{\rho_j \lambda F_j}{S_{sch}^{(c-1)}} < 1$ **then**
            if $n + x_c < N$ **then**
                $x_c \leftarrow x$
                Assign x_c resource blocks for the class-c data flow
                $n \leftarrow n + x_c$
            else
                $x_c \leftarrow (N - n)$
                Assign x_c resource blocks for the class-c data flow
                Stop allocation until next TTI
            end if
        else
            $x \leftarrow x + 1$
        end if
    end while
end for

Table 3.2 Parameter settings of smart grid traffic

Service class	1	2	3
Percentage of arrival rate	20%	30%	50%
Average requests size (bytes)	30k	50k	700k
Upper bound of scheduling time (sec)	0.001	0.003	0.007

Table 3.3 Major simulation parameters of LTE

Parameter	**Setting**
System bandwidth	10MHz
Number of RBs	50
Number of subcarriers per RB	12
RB bandwidth	180KHz
Transmission time interval	1ms
Transmission power	125mW
Noise power per Hz	160dBm
Traffic arrival model	Poisson

3.5.2 Simulation Results

Figure 3.3 shows the number of resource blocks for different classes in proposed LTE scheduling scheme. With the increase of the arriving rate, the number of allocated resource blocks is dynamically adjusted to satisfy the scheduling time requirements. For the classes with small traffic volumes, class-1 and class-2, the changes are slowly, while class-3 has a higher increase rate because of its large traffic volume.

Figure 3.4 shows the total number of resource blocks allocated in the proposed scheduling scheme is increased. In Figure 3.6 and Figure 3.7, we let the number of total resource blocks be the value shown in Figure 3.4, and perform resource allocations using the three scheduling scheme, respectively.

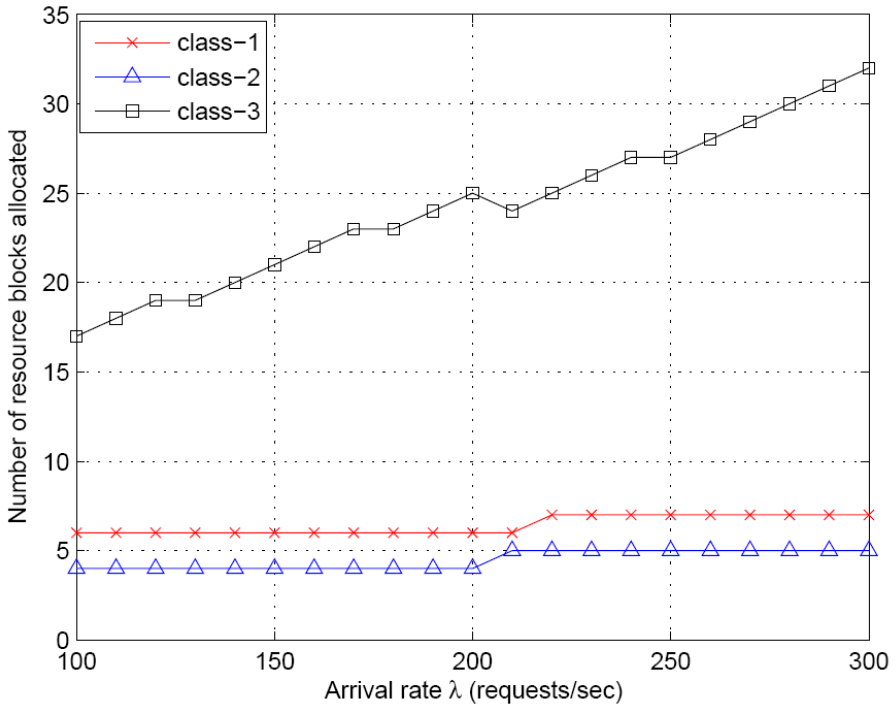

Figure 3.3 Number of resource blocks for different classes in the proposed scheduling scheme

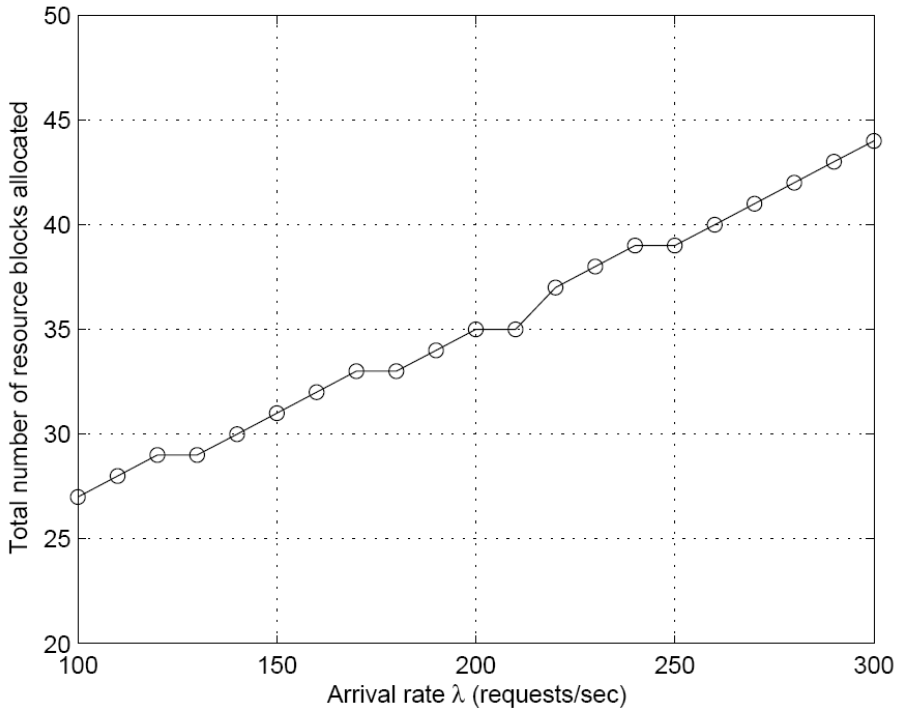

Figure 3.4 Total number of resource blocks in the proposed scheduling scheme

Figure 3.5 shows the number of allocated resource blocks for different classes among the three scheduling schemes. The totally available resource blocks for an arrival rate are the same among the three schemes. For example, when $\lambda = 150$ request/s, our proposed algorithm uses 31 resource blocks, then the other two algorithms also have 31 resource blocks available in the same arrival rate. Figures 3.6(a) to (c) show the number of resource blocks for the three classes, respectively. We can see that more resource blocks are assigned to class-1 and class-2 in Large Metric-First algorithm than our proposed algorithm. That is because the Large-Metric-First scheduling scheme is more focused on the traffic with higher priorities. In the GBR/Non-GBR scheduling scheme, class-1 and class-2 traffic flows are assigned to GBR bearers and the values do not dynamically change with the increase of arrival rate.

We can see that such kind of scheduling is inflexible. If the smart grid system encounters an emergency situation, for example, additional volume of exceptional messages, alarms and control traffic are added to the network traffic, the scheduling time performance will get much worse.

Figure 3.6 shows the scheduling time for different classes using the same amount of resource blocks indicated in Figure 3.5. The grey dash lines represent the scheduling time requirements for different classes (see Table 3.2). The Large-Metric-First scheduling and GBR/Non-GBR scheduling allocates more resource blocks to class-1 and class-2, and less resource blocks to class-3. All these three algorithms satisfy the scheduling time requirements for class-1 and class-2. But for class-3 traffic flow, the other two algorithms cannot satisfy the requirement because less resource blocks are left for class-3. The Large-Metric-First scheduling has a better performance in class-1 and class-2, while sacrificing the scheduling time in class-3. The GBR/Non-GBR can partly satisfy the requirement for class-3 when arrival rate is larger than 220 requests/sec.

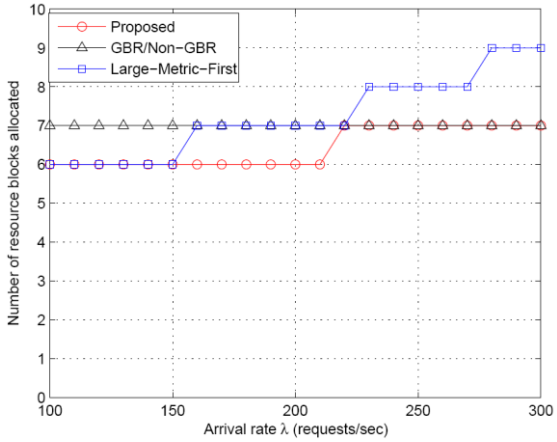

(a) Class 1

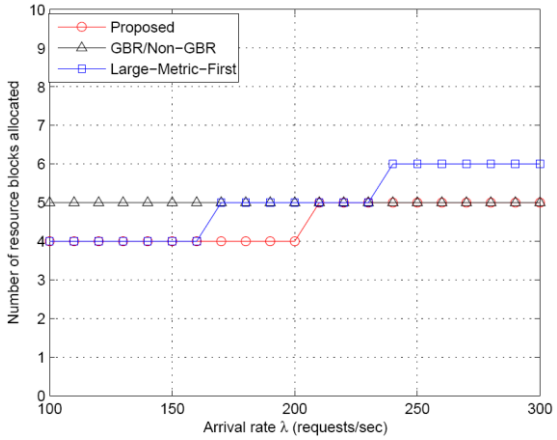

(b) Class 2

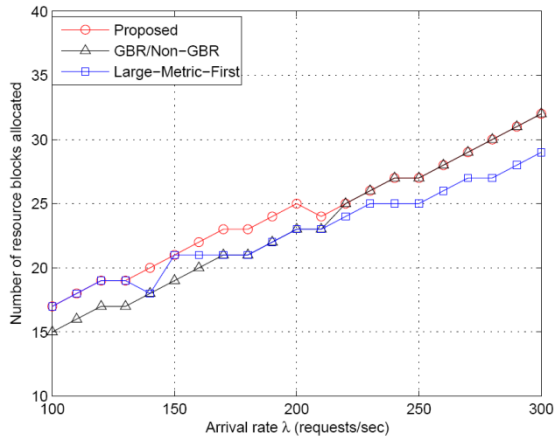

(c) Class 3

Figure 3.5 The number of allocated resource blocks for different classes

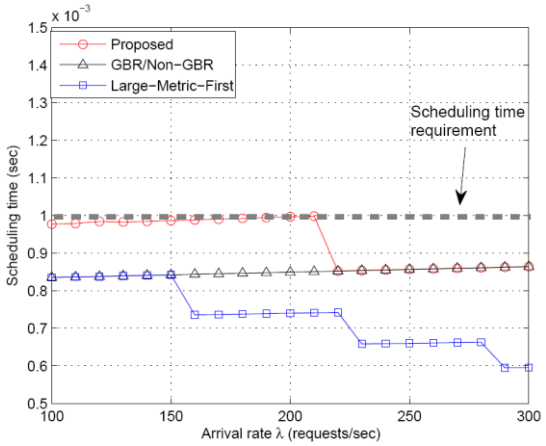

(a) Class 1

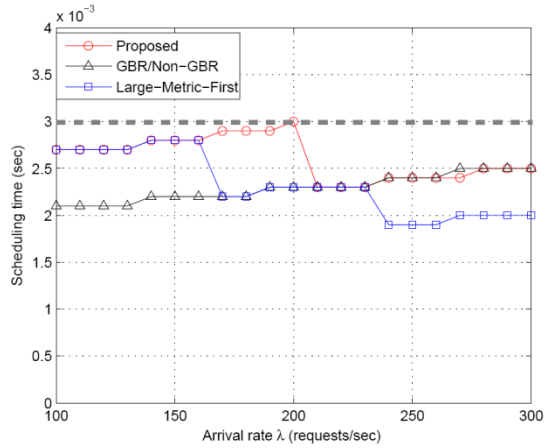

(b) Class 2

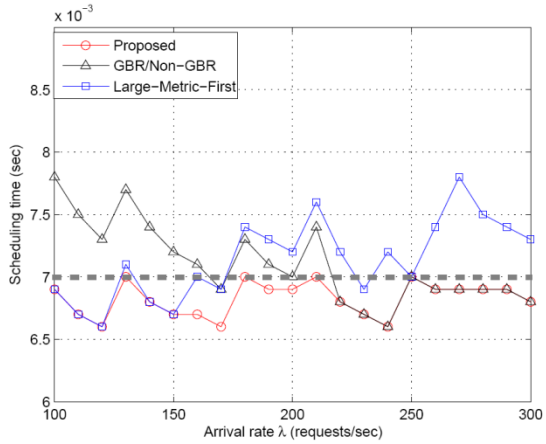

(c) Class 3

Figure 3.6 The scheduling time for different classes

3.6 Chapter Summary

In this chapter, we investigated the LTE uplink scheduling problem in smart grid WAN. We proposed an optimal scheduling algorithm for LTE in smart grid, and evaluated the scheduling time performance in smart grid network environment. The simulation results showed that the proposed algorithm is able to use less resources to satisfy the scheduling time requirement compared to the existing Large-Metric-First scheduling scheme and GBR/Non-GBR scheduling scheme.

Chapter 4
LTE load Balancing

Chapter 4 describes a new solution for LTE multi-cell load balancing in smart grid communication networks. We propose a practical load balancing algorithm to dynamically adjust the traffic load among multiple cells. The experimental results demonstrated that the proposed algorithm is able to achieve lower overall transmission delay in multi-cell LTE networks.

4.1 Introduction

In Chapter 3, we proposed a LTE uplink scheduling algorithm for smart grid communications. However, the network performance may be still deteriorated by load imbalance among multiple cells. Figure 4.1 shows a network consists of multiple cells, each of which is controlled by an eNB. Each user can receive the signal from more than one eNBs, including serving eNB (SeNB) and target eNB (TeNB). The SeNB represents the eNB which is serving the UE, while TeNB represents the eNB which can reach the UE but is not serving the UE. In a wireless cellular network, the load in different cells is time varying due to the different number of the users in each cell and the different utilization of each user. The unbalanced load among cells leads to a higher delay, and a higher packet drop rate in the higher-loaded cell, and an underutilization of resources in the lower-loaded cell.

The load balancing algorithm in the wireless cellular networks aims at finding the optimum handover operations between the overloaded cell and possible target cells. The users in the overloaded cell are handed over to the under-loaded cells in order to improve the overall network performance in terms of the latency and throughput. However, it is quite challenging to appropriately distribute the load among multiple cells for improved network performance.

The existing work on LTE load balancing has been described in Section 2.2.3. The existing methods focus on maximizing the satisfied users by satisfying the hand-over trigger requirements and reducing the traffic congestion.

In this chapter, in order to improve the network performance, we propose a load balancing scheme which can adapt to the network conditions, and achieve a better performance by appropriately distributing the load among neighbouring cells. The proposed scheme can select a proper eNB among the multiple TeNBs for each UE based on the load difference and the SINR. We conducted the performance evaluation in the network simulator OPNET. The simulation results demonstrated that the proposed scheme results in a lower end-to-end delay from the UE to the related server in case of load imbalance.

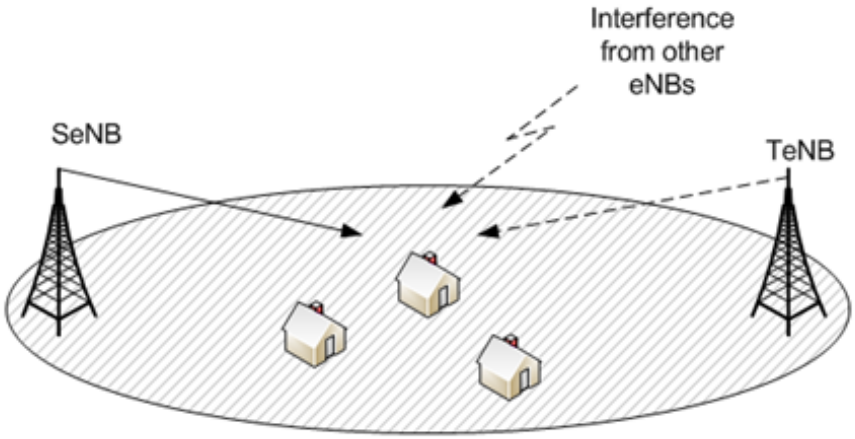

Figure 4.1 LTE network model where the UE can receive multiple signals from different eNBs

4.2 Network Models

4.2.1 Channel Model

We assume that each cell knows the instantaneous signal strength sending from its serving UEs through the control signals, such as CSI. We divide the time into time slots with equal length τ. We assume that the received SINR at eNB keeps unchanged during a time slot. The average received SINR at the base station of cell *k* from UE *i* at time slot t $SNIR_{i,k}(t)$ is given by [37]

$$SINR_{i,k}(t) = \frac{\psi_i(t)/L_{i,k}(t)}{\sum_{j\neq i}\psi_j(t)\cdot\rho_k/L_{j,k}(t)+N} \tag{4.1}$$

where $\psi_i(t)$ represents the transmit power of the UE i at time slot t, $L_{i,k}(t)$ represents path loss from the UE i to the base station k (taking into account the distance between them), and N represents the background power of Additive White Gaussian Noise (AWGN) power. ρ_k represents the RBs utilization ratio of cell k, which is described in Section 4.2.2.

The data rate $S_{i,k}(t)$ at time slot t can be calculated using Shannon-Hartley theorem, which is given in [34] as

$$S_{i,k}(t) = x_{i,k}(t)\frac{B}{N}\log_2(1+SINR_{i,k}(t)) \tag{4.2}$$

where B represents the total bandwidth for the eNB, N is the total number of RBs for each eNB, and $x_{i,k}(t)$ represents the number of RBs allocated to user i by cell k at time slot t, which can be determined using the method proposed in Chapter 3.

Therefore, the data rate depends on the channel condition between the UE and the eNB. In other words, to send the same amount of the traffic, the UE with better channel condition will consume less number of the resource blocks than the UE with worse channel condition.

4.2.2 Network Parameters

In order to investigate the different load distributions of different eNBs, we define the network parameters as follows. We use *RB utilization ratio* $\rho_k(t)$ to denote the ratio between the number of the allocated RBs and the total number of the RBs in cell *k* at time slot t. A larger $\rho_k(t)$ indicates a higher percentage of RB utilization in cell *k*, and thus a higher level of load in cell *k*. Assuming that all cells have the same number of RBs, denoted by N. Then, $\rho_k(t)$ for cell k at the time slot t can be written as [39]

$$\rho_k(t) = \frac{\sum_{i \in I} x_{i,k}(t)}{N} \tag{4.3}$$

where I represents the set of UEs in the whole network. $x_{i,k}(t)$ is the number of RBs that the cell k allocates to user i at time slot t which can be calculated by the proposed LTE uplink scheduling algorithm in Chapter 3. Here we assume that the length of the time slot τ is much larger than the subframe duration (e.g., 1 ms).

The average RB utilization ratio of the whole network at time slot t is given by

$$\rho(t) = \frac{1}{|K|} \sum_{k \in K} \rho_k(t) \tag{4.4}$$

where K is the set of the cells in the network, and $|K|$ represents the number of the cells in the set K.

The overload situation occurs when the number of RBs exceeds the amount of available RBs. However, during the handover operation, the load transfer should not exceed the capacity of the eNB. Therefore, we introduce a parameter $\xi(t)$ to indicate the load balancing level of the LTE system. The level of load balancing can be evaluated by the fairness index [40], which is given by

$$\xi(t) = \frac{[\sum_{k \in K} \rho_k(t)]^2}{|K| \, [\sum_{k \in K} \rho_k(t)^2]} \tag{4.5}$$

where the value of load balancing index $\xi(t)$ is in the range [1/N, 1]. A larger $\xi(t)$ indicates a more balanced load distribution among cells, and vice versa. Particularly, $\xi(t) = 1$ represents that all cells have equal load in time slot t.

4.3 Problem Formulation

In this section, we formulate the optimization problem for load balancing in the LTE network. On the one hand, we want to use a minimal resource to send all traffic in the network, which means that we want to minimize the average RB utilization ratio $\rho(t)$. On the other hand, we want to evenly utilize the RBs among cells, which means that we want to maximize the load balancing level $\xi(t)$. However, $\rho(t)$ and $\xi(t)$ depend on each other. Reducing $\rho(t)$ may lead to load unbalancing, while increasing $\xi(t)$ may cause a higher consumption of RBs. Considering the trade-off between the average RB utilization ratio $\rho(t)$ and the load balancing level $\xi(t)$, we introduce an *aggregation parameter z*, which is defined as

$$z = \delta\ \rho(t) - (1-\delta)\ \xi(t) \tag{4.6}$$

where δ is a weight representing the trade-off between the RB utilization and the load balancing level. If δ is set to 1, the RB utilization will be the objective. On the contrary, when δ is equal to 0, the load balancing level will be the objective. When δ is between 0 and 1, the objective is the compromised value taking into account both RB utilization and load balance.

Therefore, the optimization problem is mathematically formulated as follows:

$$\text{Minimize}_{\{x_{i,k}\}} \quad \delta\ \rho(t) - (1-\delta)\ \xi(t) \tag{4.7a}$$

Subject to:

$$\sum_{i\in I} R_{i,k}(t)\ x_{i,k}(t) \le N, \qquad \forall k \in K \tag{4.7b}$$

$$\sum_{k\in K} R_{i,k}(t) = 1, \qquad \forall i \in I, \forall k \in K \tag{4.7c}$$

$$SINR_{i,k}(t) \ge SINR_{th}, \qquad \forall i \in I, \forall k \in K \tag{4.7d}$$

The objective function (4.7a) represents the combination of the RB utilization and the load balancing level with the weight parameter, $0 < \delta < 1$. Constraint (4.7b) shows that the number of resource blocks occupied by all users in a cell should not exceed the total number of resource blocks in the cell. Constraint (4.7c) specifies that each UE can be served by only

one eNB. Constraint (4.7d) represents that a user's $SINR_{i,k}(t)$ should not be lower than the SINR threshold $SINR_{th}$ in order to ensure acceptable data communications.

4.4 Practical Load-Balancing Algorithm

The optimization problem in Equation (4.7) is an integer programming. If we use exhaust search to find the optimal solution, it is not suitable for delay-sensitive smart grid applications because the processing time will be unacceptable. In this section, we propose a practical load-balancing algorithm which provides a sub-optimal but much more efficient solution to problem in Equation (4.7). The principle of the proposed algorithm is that the UE always tries to choose an eNB with the highest z value as its serving eNB.

The proposed *Practical Load Balancing Algorithm* is executed at each SeNB. The SeNB first finds the set of the UEs, denoted by $\mathbf{S}_{UE}$, that are served by it, and then sorts the UEs in the set $\mathbf{S}_{UE}$ in an ascending order based on their SINR values. For each UE in the set $\mathbf{S}_{UE}$, SeNB will find a better TeNB if available, and hand over the UE to the chosen TeNB. The process of finding the better TeNB is as follows. First, the SeNB finds the set of the target TeNBs, denoted by W, for the current UE. Then, for each TeNB in the set W, the SeNB calculates the number of required resource blocks if the UE is handed over to the TeNB, and compares the current value z_{SeNB} with the z value of the TeNB z_{TeNB}. If the difference between z_{SeNB} and $z_{TeNB}$is larger than a threshold ρ_{th}, the UE will be handed over from the current SeNB to the TeNB. The same procedure repeats until all UEs in the set $\mathbf{S}_{UE}$ have been processed by the SeNB.

The *Practical Load Balancing Algorithm* is a sub-optimal solution to the optimization problem (4.7). The advantage of the proposed algorithm is to find the near-minimum objective at a much faster speed than the exhaust search approach. The difficulty of finding the solution to the problem (4.7) lies in the processing order of the UEs at each SeNB. UE assignments affect each other. Different processing order of UEs will lead to different results. In the *Practical Load Balancing Algorithm*, the SeNB sorts the UEs in the set $\mathbf{S}_{UE}$ in an

ascending order based on their SINR value, and process the UE with the lowest SINR value first. This method tries to transfer the UE with the worst channel condition to the TeNB with a better channel condition, which can improve the overall performance. At the same time, those UEs with better SINR keep in relatively good channel condition, because the proposed algorithm takes the fairness level into consideration.

Algorithm 2: the proposed practical load balancing algorithm executed at a SeNB

1: Find the set of UEs, denoted by $\mathbf{S}_{\text{UE}}$, that are currently served by the SeNB.
2: Sort the UEs in the set $\mathbf{S}_{\text{UE}}$ in an ascending order based on their SINR values.
3: **for** each UE in the set $\mathbf{S}_{\text{UE}}$ **do**
4: Calculate z_{SeNB} value;
5: Find the set of TeNBs, denoted by W;
6: Collect measurements (e.g., CSI) from the UE to each TeNB in the set W;
7: Obtain the number of the available resource blocks at each TeNB in the set W;
8: **for** each TeNB in the set W **do**
9: **if** $SINR \geq SINR_{th}$ **then**
10: Calculate the number of required resource blocks after the handover;
11: Calculate the z_{TeNB} value;
12: **if** $z_{SeNB} - z_{TeNB} > \rho_{th}$ **then**
13: Perform handover from SeNB to TeNB;
14: break;
15: **end if**
16: **end if**
17: **end for**
18: **end for**

If a handover is performed as long as the UEs' z value of TeNB z_{TeNB} is smaller than that of SeNB z_{SeNB}, it may lead to *handover ping-pong effect*, which means that a UE switches its SeNB frequently and cannot reach a stable state. In order to prevent the *handover ping-pong effect*, we introduce an offset value ρ_{th} in our algorithm. Only when $Z_{SeNB} - Z_{TeNB} > \rho_{th}$, the UE triggers a handover. Therefore, it is critical to define ρ_{th}. A smaller ρ_{th} may still cause the *ping-pong effect*, while a larger ρ_{th} would make the *Practical Load Balancing Algorithm* perform worse.

4.5 Simulations

OPNET Modeler [41] is a network simulation tool. It provides a comprehensive development environment for modeling and simulation of deployed wired and wireless networks. OPNET Modeler enables users to create customized models and to simulate various network scenarios. The wireless module is used to create models for wireless scenarios such as Wi-Fi and LTE. The Modeler is object-oriented and employs a hierarchical approach to model communication networks. It provides graphical user interfaces known as editors to capture the specifications of deployed networks, equipment, and protocols.

OPNET Modeler 17.1 is used to simulate the smart grid LTE WAN. OPNET provides high-fidelity modeling, simulation, and analysis of wireless networks such as interference, transmitter/receiver characteristics, and full protocol stack, including MAC, routing, higher layer protocols and applications. It also has the ability to incorporate node mobility and interconnect wire line transport networks.

4.5.1 Simulation Settings

OPNET models developed for smart grid WAN architecture in a city-scale network of 5km × 5km are shown in Figure 4.1. The scenario consists of 2 eNBs (eNodeB 1 and eNodeB 2), 8 UEs (node 1 – node 8) and a server. The eNBs are evenly located in the city area. Every 4 UEs are connected to an eNB. Node1_1 to Node 1_4 are initially connected to eNodeB_1, and Node_2_1 to Node2_4 are connected to eNodeB_2. The IP addresses assigned to Node_1_1 and Node_2_4 are 192.168.7.2 and 192.168.7.9, respectively, and the IP address of the server is 192.168.4.2. The server connects to the EPC by a link. Each UE have the same configuration in terms of the applications and the traffic volumes. The SINR threshold $SINR_{th}$ is set to 10 dB, and the system bandwidth is set to 5 MHz. We set the weight parameter δ to 0.7, which means that we pay more attention to the utilization of network resources. The topology shown in Figure 4.1 is used in load balancing evaluation and end-to-end delay evaluation.

Table 4.1 shows the traffic parameters for the OPNET simulation. Each UE sends the traffic every one second. In each time period (1 second), the UE sends 500 packets, which follow a Poisson distribution, and the packet size is 1024 bytes. Table 4.2 shows the basic LTE parameters in OPNET simulation. We assume that eNodeB_1 is the overloaded cell, and each UE of eNodeB_2 sends additional traffic according to a Poisson process with sending rate increased from 1000 kbps to 6000 kbps.

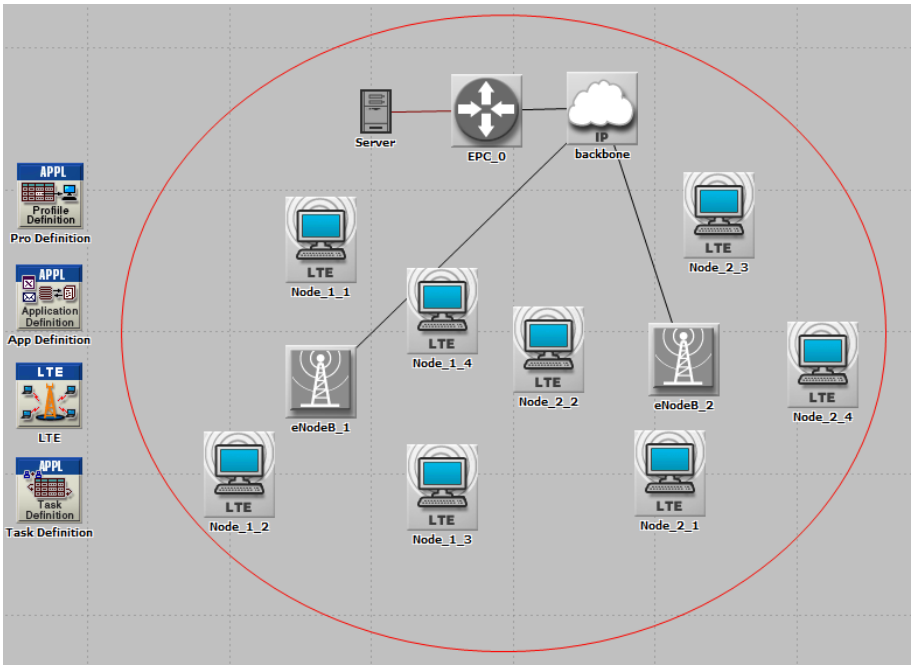

Figure 4.1 Network topology in the simulation

4.5.2 Simulation Results

4.5.2.1 Comparison between the proposed Practical Load Balancing Algorithm and the exhaust search approach

The Figure 4.2 shows the comparison of z value among the proposed Practical Load Balancing Algorithm, the exhaust search approach, and the default handover approach. The red, green, blue lines represent the proposed algorithm, the exhaust search, and the default handover, respectively. The LTE default handover approach is that the UE switches to other

eNB with the best channel condition as long as the SINR of the UE is larger than the SINR threshold. The exhaust search approach finds the optimal solution to the optimization problem (4.7) at the price of extremely high computational complexity. The proposed Practical Load Balancing Algorithm is an efficient and lightweight algorithm, which performs close to the globally optimal result, as demonstrated from the small performance gap between the proposed algorithm and the exhaust search approach in Figure 4.2. We can see that the exhaust search approach and the proposed algorithm get much lower z values than the default handover approach. Thus the proposed algorithm and exhaust search approach consume less resource and provide more balanced load for LTE system than the default handover approach.

Table 4.1 Parameter settings of traffic

Traffic sent	**Value**
Packet size (bytes)	Constant (1024)
Number of packets sent once	Poisson (500)
Initialization time (seconds)	Poisson (200)
Inter-request time (seconds)	Poisson (1)

Table 4.2 Major simulation parameters of LTE

Parameter	**Setting**
Uplink base frequency	1920 MHz
Downlink base frequency	2110 MHz
Uplink bandwidth	20 MHz
Downlink bandwidth	20 MHz

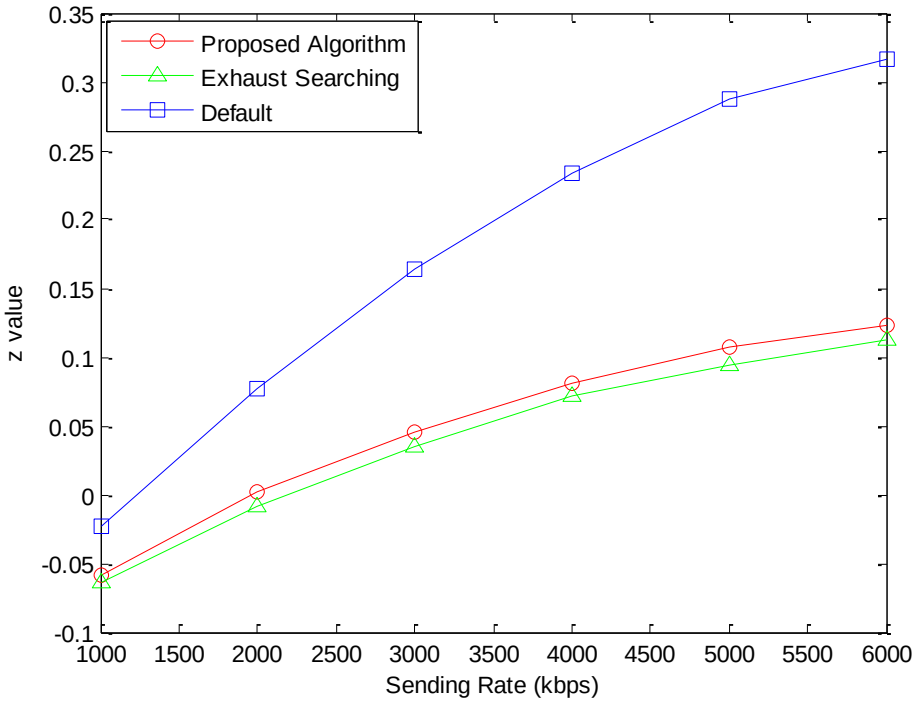

Figure 4.2 Comparison of z values among the proposed algorithm, the exhaust search approach, and the default handover approach

4.5.2.2 Load Balancing Evaluation

Figure 4.3 shows the comparison of average RB utilization ratio between the default handover approach and our proposed algorithm. The blue line represents the proposed scheme, while the red one represents the LTE default handover scheme. With the increased sending rate, both curves keep rising up, but the line of proposed algorithm is increasing slowly than the default handover scheme. The additional traffic injection from Node_1_1 to Node_1_4 makes the SINR of cell 1 worse. A worse cell would use more RBs to send the same amount of data. Through the handover, the channel conditions of the UEs become better than before. The switched UEs with better SINR consume less resource, thus leading to a lower average RB utilization ratio compared to the default handover scheme.

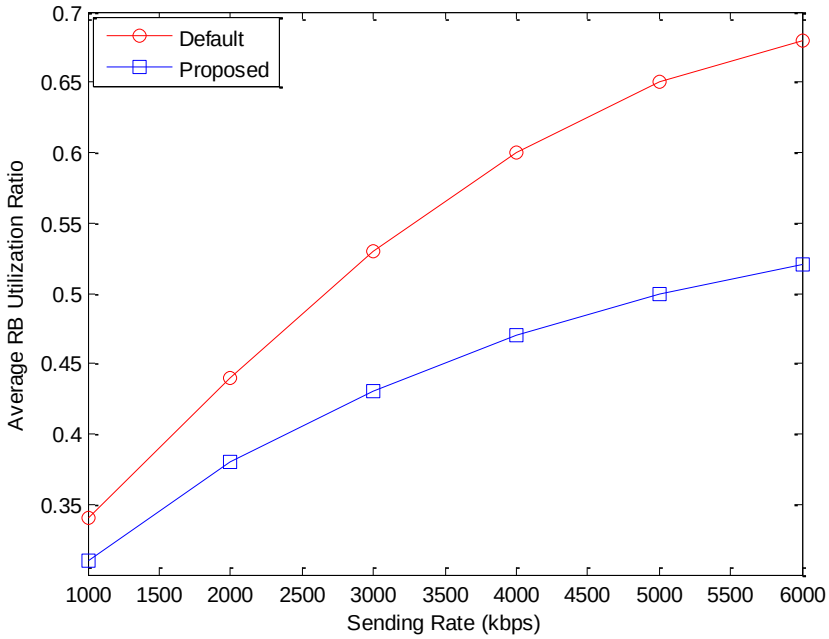

Figure 4.3 Comparison of average RB utilization ratio between the proposed algorithm and the default handover scheme

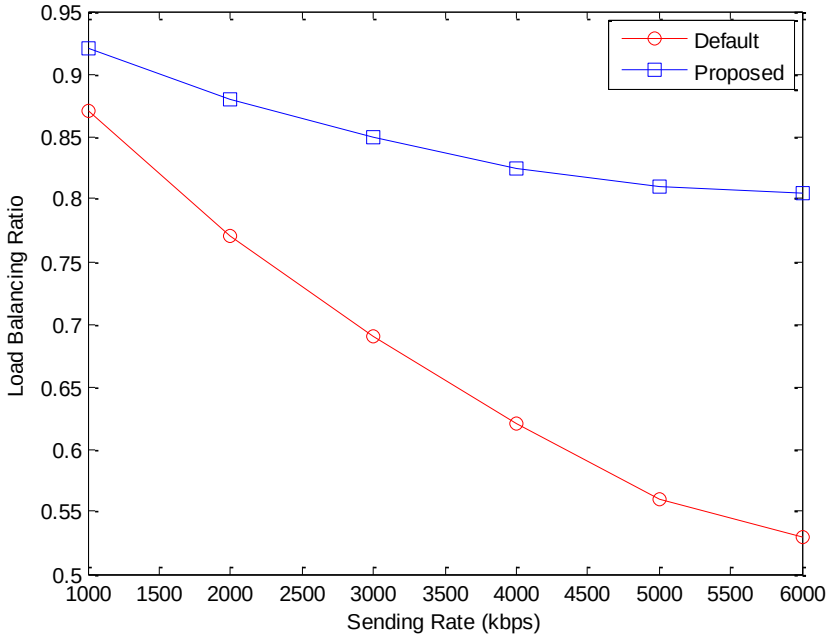

Figure 4.4 Comparison of load balancing ratio between the proposed algorithm and the default handover scheme

Figure 4.4 shows the comparison of load balancing ratio between the proposed algorithm and the default handover scheme. It is clear from the figure that the load balancing ratio for the default handover scheme reduces dramatically when the sending rate is increased. The proposed algorithm achieves a higher load balancing ratio (e.g., a more balanced load distribution) than the default handover scheme. The reason is that the proposed algorithm can appropriately transfer a part of UEs from the over-loaded cell to the under-loaded cell to balance the load.

4.5.2.3 End-to-end Delay Evaluation

Figure 4.5 illustrates the end-to-end delay between UEs and eNBs. The corresponding IP addresses of UEs and the server are shown in Table 4.3. As shown in the figure, all traffic starts after around 100 seconds. After several seconds, the values of end-to-end delays become steady. In eNodeB_1, the values remain at around 0.025 s, while in eNodeB_2, the delay values vary between 0.024 s and 0.028 s. That is due to different distances between the UEs and eNodeB, which leads to different channel conditions.

Table 4.3 IP address corresponding

Node	**IP Address**
Node_1_1	192.0.7.2
Node_1_2	192.0.7.3
Node_1_3	192.0.7.4
Node_1_4	192.0.7.5
Node_2_1	192.0.7.6
Node_2_2	192.0.7.7
Node_2_3	192.0.7.8
Node_2_4	192.0.7.9
Server	192.0.4.2

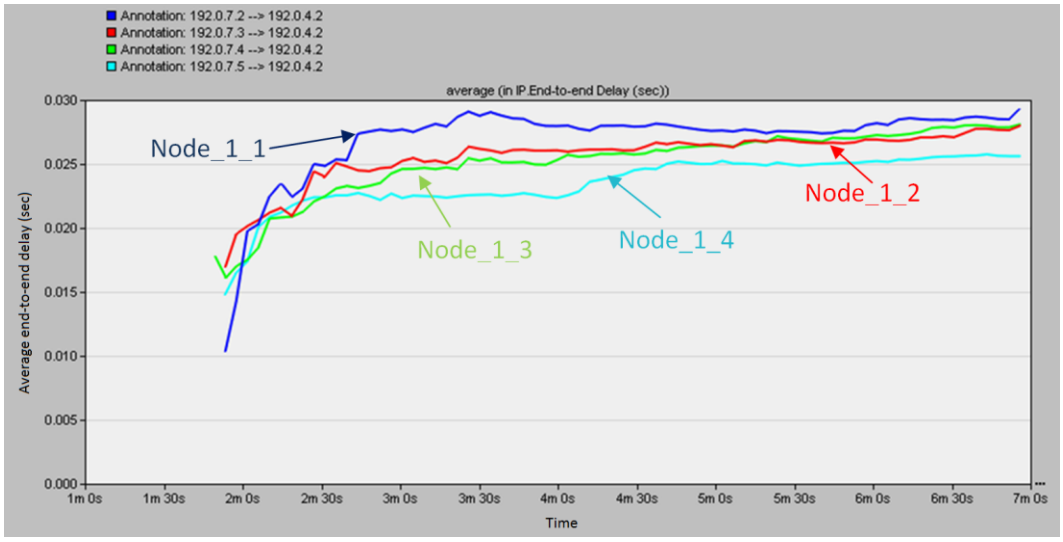

(a) End-to-end delays for Node_1_1 - Node_1_4

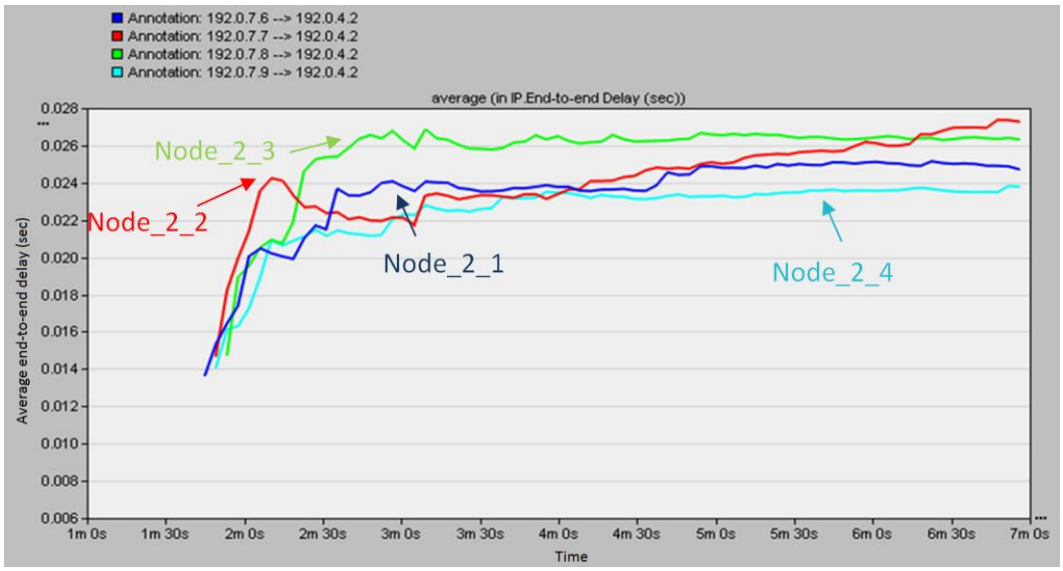

(b) End-to-end delays for Node_2_1 - Node_2_4

Figure 4.5 End-to-end delays before adding the traffic

In order to evaluate the load distribution among cells, additional traffic is added to Node_2_1, Node_2_2, Node_2_3, and Node_2_4. The additional traffic is injected at the 3rd minute from the beginning, and we observe the change of end-to-end delay before and after the traffic injection. Figure 4.6 shows the end-to-end delays of the UEs after inserting the traffic flow. As shown in the Figure 4.6(a), the UEs' delay at eNodeB_1 does not have too much change compared with the value before the traffic injection. Because the two cells are separated, the traffic injection in cell 2 does not affect the cell-1 network. Figure 4.6(b) shows the delays in default hand-over scheme, the delay values of all four nodes connected to eNodeB_2 start to increase from the third minute, and finally go above 0.04 second. The traffic injection makes the channel condition of Node_1_1, Node_1_2, Node_1_3 and Node_1_4 worse. However, the SINR values do not reach the thresholds. Therefore, the UEs do not take any hand-over action, so that the end-to-end delays are increased.

We implemented the proposed algorithm into the OPNET experiments. Figure 4.7 shows the delay values after implementing the proposed practical load balancing algorithm. When the additional traffic flow is added to eNodeB_2, the delay values of Node_2_1 to Node_2_4 start soaring, as shown in Figure 4.7(b). The increased delays are caused by the overload in eNodeB_2 when a large amount of traffic is inserted into it. When the time reaches 4 minute 20 seconds, the delay values stop increasing and start going down, as shown in Figure 4.7(b). This phenomenon occurred due to the fact that the proposed algorithm was triggered to hand over the UEs with worse channel conditions to the new SeNB, thus leading to delay reduction. In this case, Node_2_3 switches its SeNB from eNodeB_2 to eNodeB_1. After the handover, the end-to-end delays become acceptable. Node_1_1 to Node_1_4 have fluctuations at this time which are caused by the handover. With more traffic injected, the end-to-end delays soar again. At the time of 5 minute 20 seconds, the SeNB of Node_2_1 is also switched to eNodeB_1, which leads to another delay reduction in Figure 4.7(b).

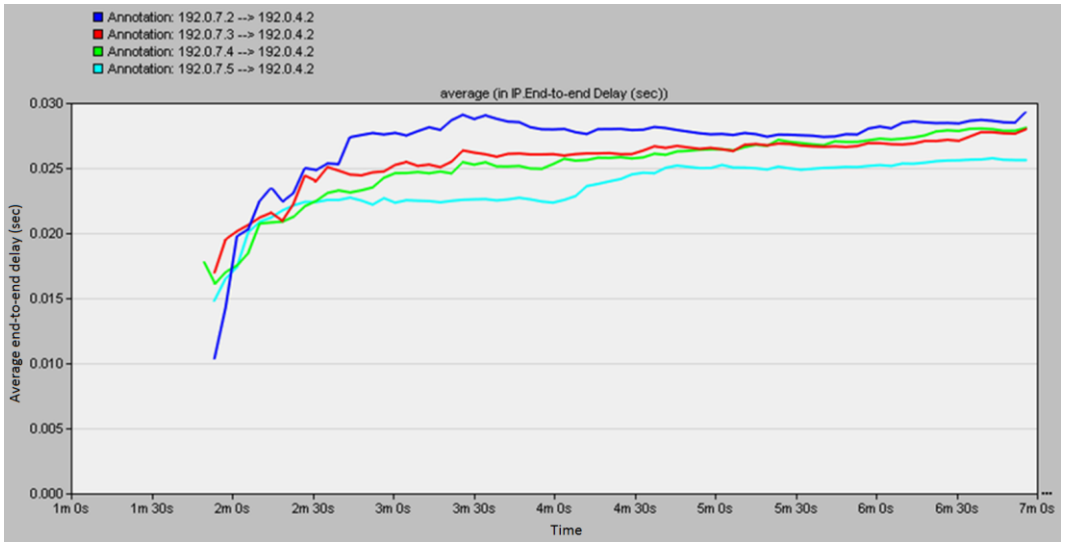

(a) End-to-end delays for Node_1_1 - Node_1_4

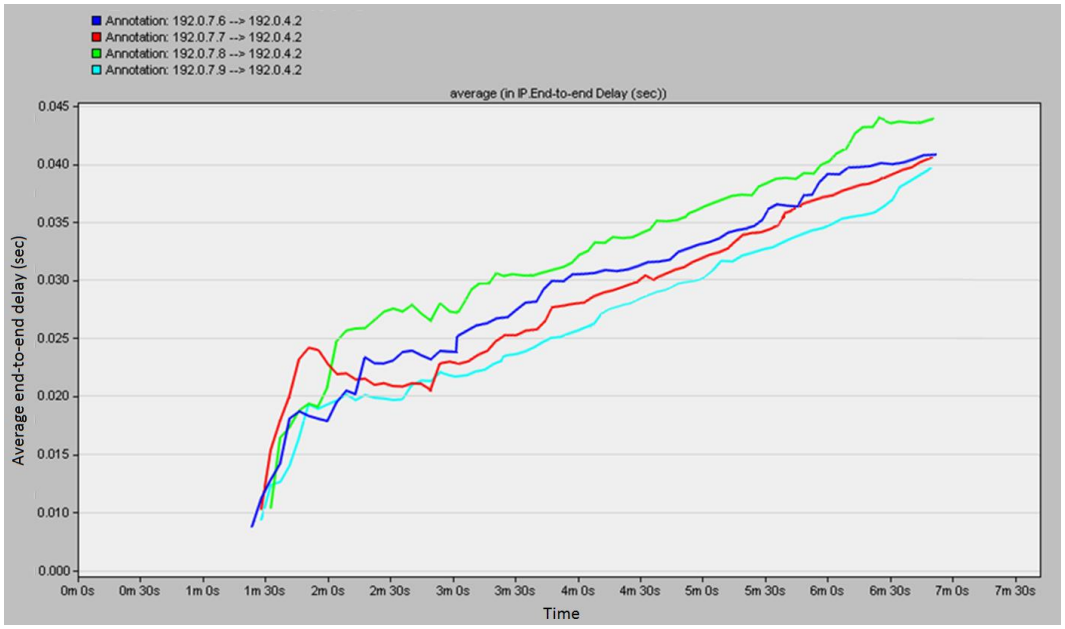

(b) End-to-end delays for Node_2_1 - Node_2_4

Figure 4.6 End-to-end delays with the default handover scheme after adding traffic flows

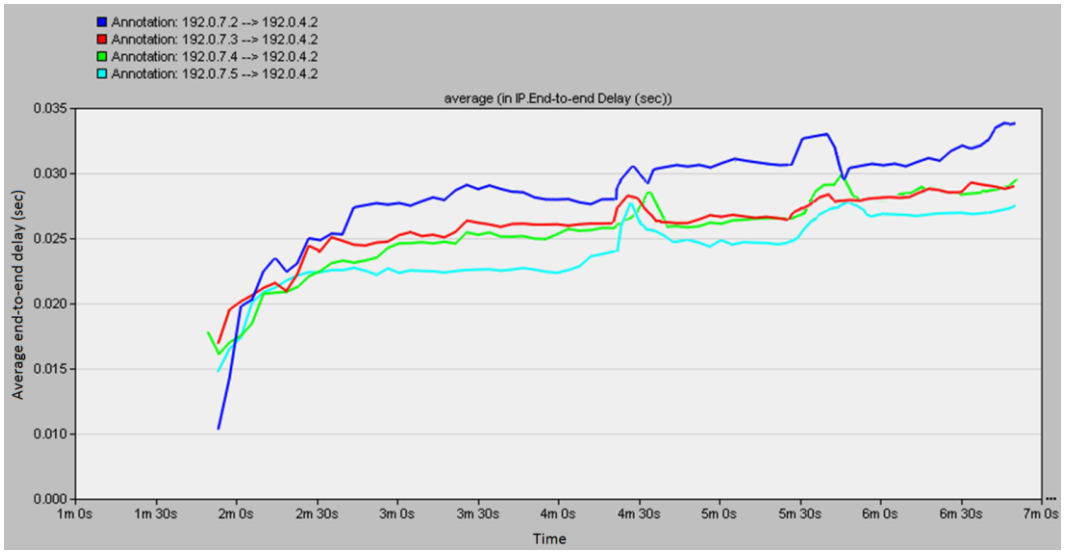

(a) End-to-end delays for Node_1_1 - Node_1_4

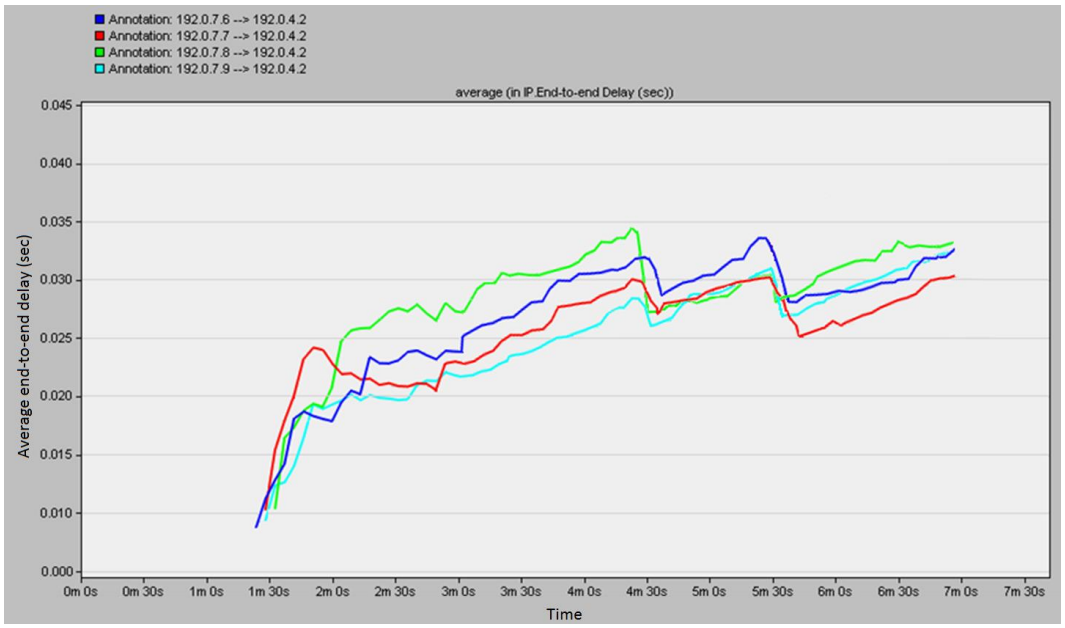

(b) End-to-end delays for Node_2_1 - Node_2_4

Figure 4.7 End-to-end delays with the proposed algorithm after adding traffic flows

Figure 4.8 shows the SeNB for each node during the experiment period. Originally, Node_1_1 to Node_1_4 are connected to eNodeB_1, and Node_2_1 to Node_2_4 are connected to eNodeB_2. Due to the additional traffic injection to eNodeB_2, Node_2_3 was handed over from eNodeB_2 to eNodeB_1 at time of 260 seconds, and Node_2_1 was handed over from eNodeB_2 to eNodeB_1 at time of 320 seconds. The handover is triggered by the proposed algorithm.

4.6 Chapter Summary

In this chapter, we investigated the LTE load balancing problem. We proposed a practical Load Balancing Algorithm for LTE to reduce the average end-to-end delay and increase the load balancing ratio. We conducted experiments in OPNET. The experiments results demonstrated that the proposed Load Balancing Algorithm led a lower delay and better load balance than the default handover scheme.

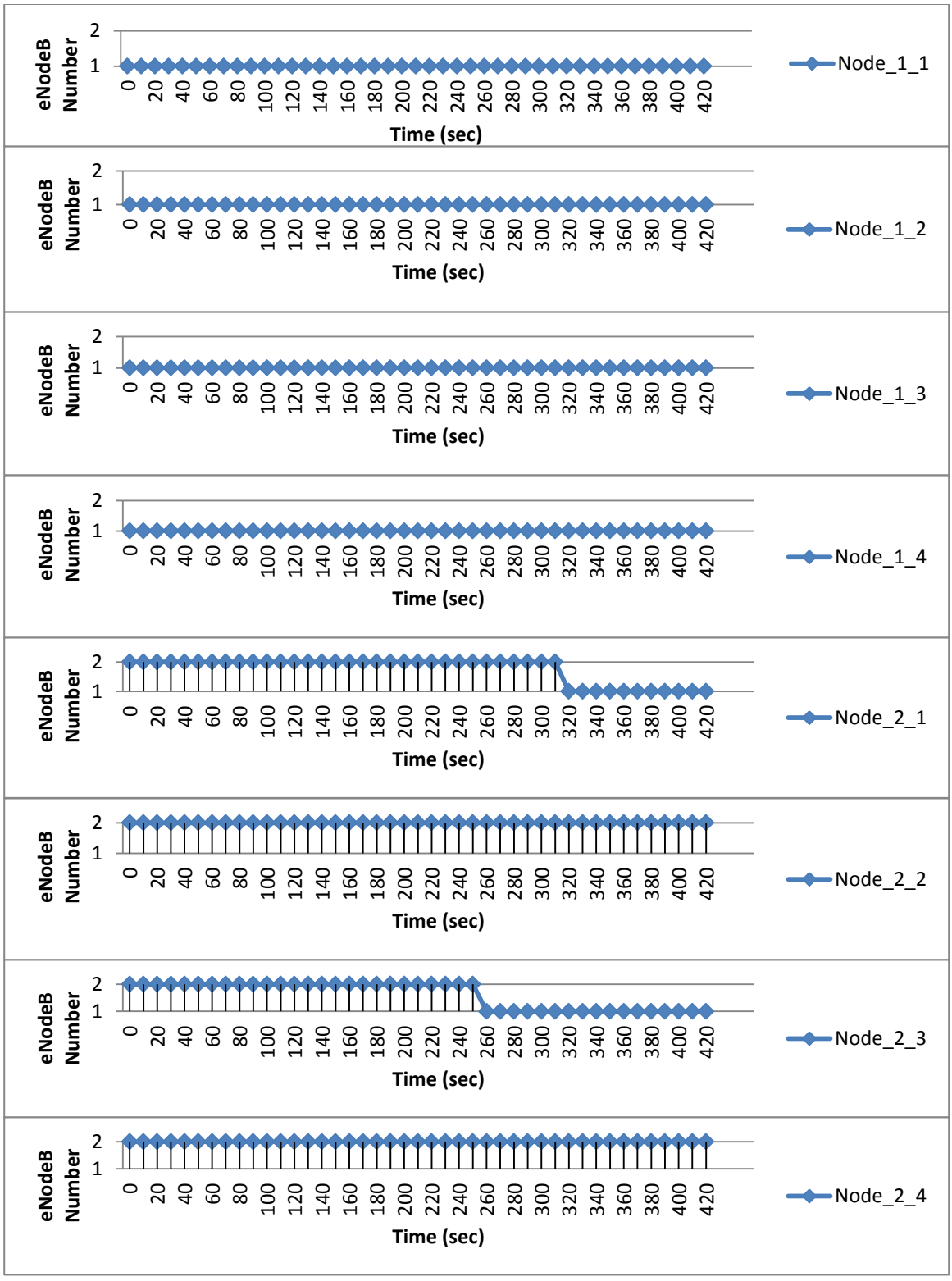

Figure 4.8 The SeNB for each node with the proposed algorithm during the experiment period

Chapter 5
Conclusion and Future Research Directions

5.1 Conclusions

In the next-generation smart grid WAN networks, the wireless communication technology will play the essential role due to its advancement and flexibility. The LTE is the promising option for smart grid because of its higher data rates, lower latency and larger coverage.

In this thesis, we proposed an optimal LTE uplink scheduling algorithm and a LTE load balancing algorithm for smart grid Wide Area Network. Latency is a critical element in smart grid networks. Many real-time smart grid applications have a low latency requirement. The presented algorithms specifically aim to reduce the transmission latency from the UEs to the LTE eNB.

Smart grid communication network consists of different classes of traffic in terms of importance, which have different QoS requirements. In LTE QoS mechanism, the scheduler acts as a key role, which defines which kind of traffic is served first and how different class of traffic should be transmitted. For this purpose, we propose a new optimal LTE uplink scheduling algorithm for smart grid WAN. Different from the existing scheduling algorithms, we apply a queuing model to calculate the scheduling time of the scheduling process. Based on different scheduling time requirements for different classes of traffic, the resource blocks

are allocated to different users in a differentiated way. The proposed scheduling algorithm can utilize the minimal resource to satisfy the scheduling time requirements for different classes of traffic. The simulation results demonstrated that the proposed scheduling algorithm outperforms the existing scheduling algorithms in terms of resource utilization.

In LTE networks with multiple cells, load imbalance may cause congestions. Therefore, it is crucial to appropriately distribute the load among cells. We formulate the load balancing problem in multi-cell LTE networks, considering both the resource utilization ratio and the load balancing level. We proposed a practical Load Balancing Algorithm to solve the load balancing problem. The experimental results in OPNET demonstrated that the proposed load balancing algorithm can obtain a lower average end-to-end delay and a better load balance than the default handover scheme.

5.2 Future Research Directions

The thesis is based on 3GPP LTE standards Release 8, which has been deployed in industry in many countries. While the newer release-LTE Release 9 or even LTE-Advanced standards are currently under development. The newer standards provide higher performance than Release 8 (for example, data rate). LTE-advanced also adds new features such as relay-based networking, which greatly enlarge the coverage of the signal and optimize the load balancing mechanism. In the near future, the research attention will be focuses on the newer LTE standard for smart grid communications.

Moreover, the models proposed in this thesis can be further developed and enhanced to give a more comprehensive and accurate representation for the LTE network.

Bibliography

[1] L. B. Le and T. Le-Ngoc, "QoS provisioning for OFDMA-based wireless network infrastructure in smart grid," in *proc. of IEEE Electrical and Computer Engineering 2011 24th Canadian Conference on CCECE*, pp. 813-816, May 2011.

[2] Y. Kim and M. Thottan, "SGTP: smart grid transport protocol for secure delivery periodic real time data," *Bell Labs Technical Journal*, vol. 16, no. 3, pp. 83-99, Dec 2011.

[3] O. C. Onar, M. Starke, G. P. Andrews and R. Jackson, "Modeling, controls, and applications of community energy storage systems with used EV/PHEV batteries," in *proc. of IEEE Transportation Electrification Conference and Expo (ITEC)*, June 2012.

[4] B. P. Roberts and C. Sandberg, "The role of energy storage in development of smart grids," *Proceedings of the IEEE*, vol. 99, no. 6, pp. 1139-1144, June 2011.

[5] P. Cheng, L. Wang, B. Zhen and S. Wang, "Feasibility study of applying LTE to smart grid", *in proc. of Smart Grid Modeling and Simulation (SGMS), 2011 IEEE First International Workshop*, pp. 108-113, Oct 2011.

[6] B.A. Bjerke and QUALCOMM INC, "LTE-advanced and the evolution of LTE deployments", *IEEE Wireless Communications*, vol. 18,no. 5, pp. 4-5, Oct 2013.

[7] Smart Grid = Information and Communication Technologies. [Online]. Available: http://www.ic.gc.ca/eic/site/028.nsf/eng/00382.html

[8] A. Ghosh and R. Ratasuk, *Essentials of LTE and LTE-A*, Cambridge University Press, July 2011.

[9] H. Holma and A. Toskala, *LTE for UMTS - OFDMA and SC-FDMA based radio access*, John Wiley and Sons, 2009.

[10] 3GPP TS 36.101: “Evolved Universal Terrestrial Radio Access (E-UTRA); User Equipment (UE) radio transmission and reception”, 3GPP, ver. 8.7.0, rel. 8, 2009.

[11] J. Ekanayake, N. Jenkins, K. Liyanage, J. Wu and A. Yokoyama, *Smart grid: technology and applications*, John Wiley & Sons, 2009.

[12] V.C. Gungor, B. Lu, and G.P. Hancke, "Opportunities and challenges of wireless sensor networks in smart grid." *IEEE Transactions on Industrial Electronics, vol.* 57, no. 10, pp. 3557-3564, Feb 2010.

[13] A. Aggarwal, S. Kunta, and P.K. Verma. “A proposed communications infrastructure for the smart grid,” in *proc. of IEEE Innovative Smart Grid Technologies (ISGT),* Jan 2010.

[14] O. Delgado and B. Jaumard, “Scheduling and resource allocation in LTE uplink with a delay requirement,” in *proc. of 2010 IEEE Eighth Annual Communication Networks and Services Research Conference (CNSR),* pp. 268-275, May 2010.

[15] F.D. Calabrese, C. Rosa, K.I. Pedersen and P.E. Mogensen, “Performance of proportional fair frequency and time domain scheduling in LTE uplink,” In *proc. of 2009 IEEE European Wireless Conference*, pp. 271-275, May 2009.

[16] Y. Xu, and C. Fischione, “Real-time scheduling in LTE for smart grids,” in *proc. of 2012 5th IEEE International Symposium on Communications Control and Signal Processing (ISCCSP)*, May 2012.

[17] E. Yaacoub and Z. Dawy, “A game theoretical formulation for proportional fairness in LTE uplink scheduling,” in *proc. of 2009 IEEE Wireless Communications and Networking Conference*, Apr 2009.

[18] S.N.K. Marwat, T. Weerawardane, Y. Zaki, C. Goerg and A. Timm-Giel, “Performance evaluation of bandwidth and QoS aware LTE uplink scheduler,” *Wired/Wireless Internet Communication*, pp. 298-306, 2012.

[19] M. Anas, C. Rosa, F. Calabrese, K. Pedersen and P. Mogensen, “Combined admission control and scheduling for QoS differentiation in LTE uplink,” in *proc. of 2008 IEEE 68th Vehicular Technology Conference*, Sept 2008.

[20] S. Ali, M. Zeeshan and A. Naveed, "A capacity and minimum guarantee-based service class-oriented scheduler for LTE networks," *EURASIP Journal on Wireless Communications and Networking*, Mar 2013.

[21] Z. Li, C. Yin and G. Yue, "Delay-bound power-efficient packet scheduling for uplink systems of LTE," in *proc. of 2009 5th International Conference on Wireless Communications, Networking and Mobile Computing*, pp. 339-345, Sept 2009.

[22] F. Sokmen and T. Girici, "Uplink resource allocation Algorithms for Single Carrier FDMA systems," in *proc. of 2010 IEEE European Wireless Conference,* pp. 339-345, Apr 2010.

[23] I. Viering, M. Dottling and A. Lobinger, "A mathematical perspective of self-optimizing wireless networks," in *proc. of 2009 IEEE International Conference on Communications*, June 2009.

[24] A. Lobinger, S. Stefanski, T. Jansen, and I. Balan, "Load balancing in downlink LTE self-optimizing networks," in *proc. of 2010 IEEE 71st Vehicular Technology Conference (VTC 2010-Spring),* May 2010.

[25] K.A. AliHossam H.S. Hassanein and H.T. Mouftah, "Directional cell breathing based reactive congestion control in WCDMA cellular networks," in *proc. of 2007 IEEE 12th Symposium on Computers and Communications (ISCC)*, pp. 685-690, July 2007.

[26] Y. Yang, P. Li, X. Chen and W. Wang, "A high-efficient algorithm of mobile load balancing in LTE system," in *proc. of 2012 IEEE Vehicular Technology Conference*, Sept 2012.

[27] 3GPP TS 36.321, "Evolved Universal Terrestrial Radio Access (E-UTRA); Medium Access Control (MAC) Protocol Specification," 3GPP, ver. 8.12.0, rel. 8, Mar 2012.

[28] Yan, Ye, Yi Qian, Hamid Sharif and David Tipper, "A survey on smart grid communication infrastructures: Motivations, requirements and challenges," *IEEE Communications Surveys & Tutorials*, vol. 15, no. 1, pp. 5-20, Feb 2012.

[29] A. Aggarwal, S. Kunta, and P.K. Verma. "A proposed communications infrastructure for the smart grid," in *proc. of IEEE Innovative Smart Grid Technologies (ISGT),* Jan 2010.

[30] V.C. Gungor, D. Sahin, T. Kocak, S. Ergut, C. Buccella, C. Cecati and G.P. Hancke. "Smart grid technologies: communication technologies and standards," *IEEE transactions on Industrial informatics,* vol. 7, no. 4, pp. 529-539, Nov 2011.

[31] Electric Power Research Institute (EPRI), "Report to NIST on the Smart Grid interoperability standards roadmap," Aug 2009.

[32] Z. Feng, J. Liu and Y. Zhang, "Study on the application of advanced broadband wireless mobile communication technology in smart grid," in *proc. of 2010 IEEE International Conference on Power System Technology (POWERCON)*, Oct 2010.

[33] D. Gross and C. M. Harris, *Fundamentals of queuing theory*, Wiley, 1998.

[34] M. M. Tantawy, A. S. T. Eldien and R. M. Zaki, "A novel cross-layer scheduling algorithm for Long Term-Evolution (LTE) wireless system," *Canadian Journal on Multimedia and Wireless Networks,* vol. 2, no. 4, pp. 57-62, Dec 2011.

[35] 3GPP TR 36.942: "ETSI TR 136 942; LTE; evolved universal terrestrial radio access(E-UTRA); radio frequency (RF) system scenarios," 3GPP, ver. 9.3.0 Rel. 9), 2012

[36] H. Safa and K. Tohme, "LTE uplink scheduling algorithms: performance and challenges," in *proc. of 2012 IEEE 19th International Conference on Telecommunications*, Apr 2012.

[37] J. G. Andrews, R. K. Ganti, M. Haenggi, N. Jindal and S. Weber, "A primer on spatial modeling and analysis in wireless networks," *IEEE Communications Magazine*, vol. 48, no. 11, pp. 156--163, 2010.

[38] M. Alasti, B. Neekzad, J. Hui, R. Vannithamby, "Quality of Service in WiMAX and LTE networks [topics in wireless communications]," in *proc. of 2010 IEEE International Conference on Communication Systems (ICCS)*, vol. 48, no. 5, pp. 104-111, May 2010.

[39] Z. Li, H. Wang, Z. Pan, N. Liu and X. You, "Joint optimization on load balancing and network load in 3GPP LTE multi-cell networks," in *proc. of 2011 IEEE International Conference on Wireless Communications and Signal Processing (WCSP),* Nov 2011.

[40] D. Chiu and R. Jain, "Analysis of the increase and decrease algorithms for congestion avoidance in computer networks," *Computer Networks and ISDN Systems*, vol. 17, no. 1, pp. 1-14, Jun 1989.

[41] OPNET Modeler network simulation software [Online]. Available: www.opnet.com.